communications materials

REVIEW ARTICLE

https://doi.org/10.1038/s43246-023-00391-2 OPEN

Multiscale mechanics and molecular dynamics simulations of the durability of fiber-reinforced polymer composites

Kui Lin [1]✉ & Zhanlong Wang [2]✉

Fiber-reinforced polymer (FRP) composites have gained widespread applications in many engineering fields, making it imperative to study long-term performance under service conditions. Due to their heterogeneity and multifield coupling conditions, the long-term performance of FRP composites has become a complex scientific problem that involves multiscale and multidisciplinary aspects. With advancements in nanotechnology and computational power, researchers have increasingly conducted studies on the deterioration mechanisms and durability of FRP composites using top-down experiments and bottom-up multiscale simulations. Here, we review micro- and nano-mechanics in relation to the durability of FRP composites, including progress in the use of atomic and molecular simulations. We elucidate the role of multiscale methods, particularly molecular dynamics simulations, in the study of FRP composites and outline its prospects, to illustrate how micro- and nano-mechanics contribute to research on the durability of FRP composites.

Fiber-reinforced polymer (FRP) composites have been widely used in aviation/aerospace structures[1], shipbuilding, and other industrial fields due to their good corrosion resistance, high strength-to-weight ratio, and strong designability. These inherent advantages have propelled FRP composites towards becoming a pivotal reinforcement material in civil engineering[2,3] and have been increasingly used in new construction[4–6] over the past two decades. However, the ability of FRP composites to resist damage during long-term service, i.e., durability, in the face of complex service environments has become one of the most important scientific issues in the field of engineering.

The study of material damage is closely related to surface/interface issues, particularly for FRP composites, which are characterized by the interfaces between fibers and the polymer matrix. Therefore, an appropriate interface model that transfers the results obtained from atomic/molecular simulations to continuous medium simulation is essential for achieving cross-scale modeling. Additionally, microscopic defects such as bubbles and voids are inevitably introduced during the production process of FRP composites[7]. Even pure epoxies (e.g., amine-cured epoxies) contain nanopores that enable the transport and storage of moisture[8]. Given the various service conditions, FRP composites may be subjected to a combination of different environmental loads (e.g., ultraviolet radiation from sunlight; freeze-thaw cycles; diurnal/seasonal temperature changes; moisture from humidity, rainfall, immersion, or seawater; and alkaline solutions from concrete pore water)[9]. These external environments, particularly when combined with the aforementioned microstructures, may lead to the deterioration of FRP composites, ultimately impacting their durability. Hence, there is an urgent need to investigate the microscopic mechanism, identify a suitable coupling method, and integrate cross-scale simulations to achieve a quantitative explanation of the macroscopic phenomenon of deterioration.

[1] Department of Civil and Environmental Engineering, The Hong Kong Polytechnic University, Hung Hom, Kowloon, Hong Kong, China. [2] Shenzhen Institute of Advanced Technology, Chinese Academy of Sciences, Shenzhen 518000 Guangdong, China. ✉email: kui-cee.lin@polyu.edu.hk; zl.wang1@siat.ac.cn

With the advancement of experimental technology and simulation methods below the microscale[10], an increasing number of researchers are attempting to explain the corresponding macroscopic phenomena from a microscopic perspective. In experiments, scanning electron microscopy (SEM) and transmission electron microscopy (TEM)/high-resolution TEM have been used to observe the microstructure of FRP composites[11–14], such as fiber-matrix interfaces, microcracks, voids in a matrix, etc. The fine details of microstructure provide an intuitive reference for computational modeling and understanding of the deterioration mechanism of materials. Atomic force microscopy (AFM) has been used to investigate the microstructure and mechanical properties of FRP composites[15,16], such as the local modulus of the sample. X-ray computed tomography (CT) can non-invasive capture the three-dimensional structure of the material[17,18] and provide the internal pore distribution and porosity, as well as generate a three-dimensional model for simulation or mechanical performance analysis. The glass transition temperature (T_g) and thermodynamic properties of epoxy can be determined by differential scanning calorimetry (DSC)[12,14]. X-ray photoelectron spectroscopy (XPS), Fourier transform infrared spectroscopy (FTIR), and Raman spectroscopy are available to characterize and analyze the changes in the chemical components and molecular structure of FRP composites under different environmental conditions[11,12,14,19], such as functional group and hydrogen bond. These experimental methods not only offer direct evidence for understanding the microscopic mechanisms but also provide reference and comparison for modeling and analysis of simulations, thus enabling the understanding of microscopic mechanisms from the atomic scale to the macroscale.

Multiscale simulation methods have been developed gradually, such as density functional theory (DFT), ab initio molecular dynamics (AIMD), reactive force field (e.g., ReaxFF) MD, classical MD, coarse-grained (CG) MD, Monte Carlo (MC) method, phase field method, finite element method (FEM), etc. The multiscale covers the atomic scale, nanoscale, mesoscale (or microscale), and macroscale (> 10^{-3} m) as shown in Fig. 1, with this paper focusing on the scale that ranges from the atomic scale to the mesoscale. It should be noted that there is currently no uniform division of different scales and no absolute boundary between adjacent scales but a transitional area[20], and this paper only divides the scale characteristics of FRP composites. Different theories and methods are required to deal with issues at different scales. At the atomic scale, quantum effects and charge transfer need to be considered, such as in the cross-linking reaction of polymer curing, material corrosion, and other chemical reactions. At the nanoscale, issues related to nano mechanics are considered, including nonbonding interactions (i.e., van der Waals interaction and hydrogen bond). For example, the adhesion between polymeric matrix and fibers mainly involves nonbonding interactions, and only a few specially treated fibers are additionally bonded by chemical bonds[21,22]. The mesoscale is where continuum mechanics and nano mechanics converge[20]. At the mesoscale, defects, interfaces, and nonequilibrium characteristics are common. The formation of microcracks and voids all involve interface problems, and the problems of voids in FRP composites are particularly important at the mesoscale. At this scale, more attention is paid to the problem of multifield couplings, such as the changes in the internal structure and mechanical properties of FRP composites under coupling effects of moisture, seawater, temperature, and voids. For instance, in a humid environment, water enters the interior of the FRP composite due to capillary action and diffusion, which affects the properties of the matrix and interface[23]. The most common macroscale methods are FEM simulations and experiments, which are widely used in the study of mechanical properties, and many models have been established in the study of FRP composites. In cross-scale modeling, the transfer of physical quantities in the transition area is a critical issue.

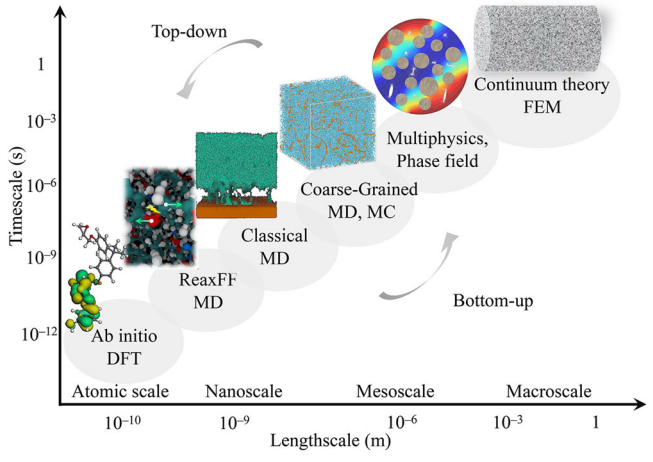

Fig. 1 Multiscale simulation framework of FRP composites. It describes a bottom-up approach that comprises Ab initio, DFT, ReaxFF MD, Classical MD, CGMD, MC, Phase field, and FEM simulation methods and displays the time and length scales corresponding to each simulation method along with the corresponding schematic models.

MD simulation has played a crucial role in bridging the gap between quantum chemistry and continuum mechanics, as shown in Fig. 1. It is a fundamental and versatile tool that can simulate the molecular structure and investigate the mechanical, chemical, and thermodynamic properties of materials from the atomic/molecular level. However, as MD simulations use a single atom or molecule as the simulation unit, the trajectory of all particles in phase space must be obtained by solving the Hamiltonian equation of the entire system, leading to extensive calculations and limiting the size of the simulation system. Macroscale failure or debonding of the structure is a large-scale disaster that involves a large time and spatial scale. As a result, establishing a direct relationship between nano/microscopic results and macroscopic phenomena is a challenge for MD simulation. Bridging the nano/microscale and the macroscale is both a challenge and an opportunity for interdisciplinary research. To this end, many research teams have proposed multiscale research methods to overcome the limitations of MD simulation[24–26].

This review first provides a brief overview of the interdisciplinary and multiscale problems encountered in the study of the durability of FRP composites. It discusses the various factors, such as temperature, ultraviolet radiation, humidity, seawater, and corrosive action, that influence the properties of FRP composites, leading to thermodynamic, mechanical, chemical, and multifield coupling problems. It also introduces the accelerated method for durability testing and its applicable conditions. Since the deterioration of FRP composites during service involves interface problems, such as debonding, fracture, and delamination, two typical interface models are introduced. To understand the durability and deterioration mechanism of FRP composites from the nano/microscale perspective, the review introduces related physical and mechanical issues, such as van der Waals interaction, hydrogen bond interaction, disjoining pressure, and capillary action. After introducing these interdisciplinary backgrounds and foundations, the methods of bridging length and time scales in the durability studies of FRP composites are reviewed. It mainly introduces related multiscale simulation methods and their corresponding theories, as well as the physical parameters available at each length scale. MD simulations have

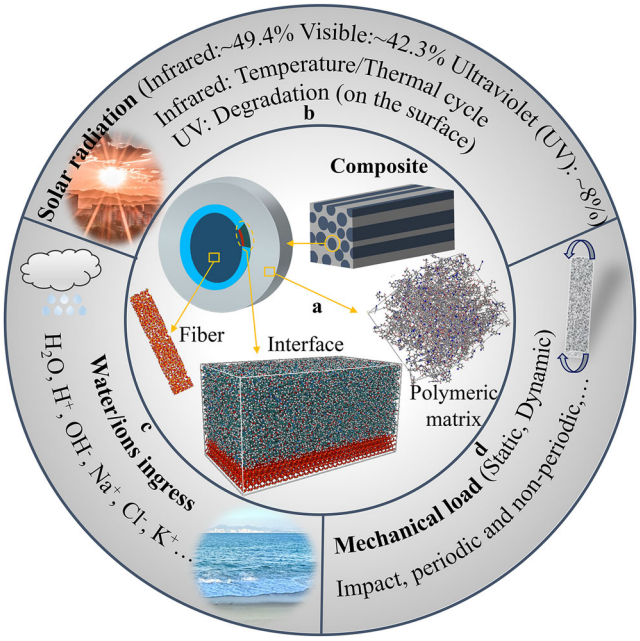

Fig. 2 Representative service environments for FRP composites. **a** Schematic diagram of the microstructural components of FRP composites. Representative service environments: **b** solar radiation, **c** water/ions ingress, and **d** mechanical load.

played a bridge role between quantum chemistry and continuum mechanics in multiscale modeling. Therefore, the review provides a detailed overview of atomic- and molecular-scale simulations of FRP composites, including ReaxFF MD, classical MD, and CG MD, in the study of their mechanical properties and durability. Moreover, the review briefly introduces the problem of multiscale voids in FRP materials. While it is impossible to cover all advances in the field of micro- and nano-research of FRP composites in a single paper, this review focuses on a few typical topics of the vast subject. Due to the complexity of the subject and the limited knowledge of the authors, there may be inevitably neglected topics and deficiencies. Nonetheless, the main purpose of this review is to clarify the role of multiscale simulation methods, especially MD simulations, in FRP composite research and outline its prospects, hoping to illustrate how micro- and nano-mechanics contribute to FRP durability research.

Interdisciplinary and multiscale problems in the durability studies of FRP composites

Multifield coupling. The laws of the life-cycle temporal-spatial evolution and the durability of FRP composites under multiple environmental effects (see Fig. 2b–d) are crucial scientific issues. Revealing the fatigue and creep damage evolution laws of FRP composites in the life cycle with multifield couplings (e.g., high and low-temperature cycles, ultraviolet radiation, corrosive environment, and repeated/sustained loads)[27,28] are urgently needed. In this section, typical environmental effects, including temperature, ultraviolet, water, and seawater are briefly introduced.

Thermal effects. Sunlight generates both thermal and photochemical effects, as shown in Fig. 2b. The thermal effect of sunlight is mainly generated by the infrared part. Temperature reflects the macroscopic expression of the thermal motion of particles, such as atoms, ions, and molecules. Changes in the temperature of a system can alter the equilibrium status or relative position of particles, leading to macroscopic manifestations such as glass transition or rubberization, thermal stress, and expansion or contraction. High energy levels of particle movement can break chemical bonds, such as in combustion and pyrolysis.

Under real conditions, the thermal effect of solar radiation is directional and produces a thermal gradient, which may cause different parts of the polymer material to expand and contract at different rates, thereby generating internal stress and destroying the material. Higher temperatures also accelerate the diffusion rate of water or salt ions in epoxy. Exposure experiments demonstrated that, in the first week, the water absorption rate in samples conditioned at 60 °C was higher than in those conditioned at 30 °C[29]. Schutte et al. found evidence that the increased water content degrades the interface strength of the glass fiber-reinforced polymer (GFRP)[30]. Additionally, water adsorption in a polymer can cause plasticization and decrease the T_g[31–33]. Hence, ambient temperature also affects the T_g by accelerating the diffusion and adsorption of water. In addition to being affected by water adsorption plasticization, the initial T_g of epoxy strongly depends on the curing temperature[34]. According to Dai et al.[35], the interfacial fracture energy remains almost constant initially and subsequently begins to decrease as the temperature approaches the T_g of the bonding adhesive. This finding suggests that the curing temperature also indirectly affects the critical temperature at which the interfacial fracture energy starts to change. In general, the temperature can not only generate thermal stress and cause plasticization during service but also affect the important thermal property parameter (i.e., T_g) of a cured adhesive[36] in various ways (e.g., effect by ambient temperature and curing temperature), which ultimately affects the mechanical properties and durability of FRP composites.

Photochemical effect. The photochemical effect is mainly generated by the ultraviolet (wavelength $\lambda = 295 \sim 380$ nm) part of sunlight. According to the bond dissociation energy, the maximum sensitivity wavelength of some polymers is in the range of 290 ~ 400 nm[37]. Hence, the absorbed ultraviolet light can produce the energy ($\Delta E = hc/\lambda$, where h is Planck's constant, and c is the velocity of light) required to break certain chemical bonds of the polymer[38]. Exposure to combined ultraviolet light and thermal shock may reduce the mechanical strength of an epoxy adhesive[39–42]. Researchers also found that the tensile strength of epoxy is reduced by 13.9% upon ultraviolet exposure, while this exposure does not influence the tensile strength of carbon fiber-reinforced polymer (CFRP) composites[42]. Additionally, ultraviolet light cannot deeply penetrate the composites, and only the irradiated surface of the composites is damaged[40]. In contrast to the temperature effect of solar radiation, which can conduct thermal energy to the interior, the photochemical effect of solar radiation only affects the outer layer of FRP composites. However, direct exposure of FRP to sunlight couples the two effects, leading to a more complex situation.

Corrosive effect. The influence of corrosive environments on composites made of epoxy resins has been investigated by many researchers[43–46]. Wu et al. performed experimental studies on the tensile properties of basalt fiber, epoxy, and basalt fiber-reinforced polymer (BFRP) composites in different corrosive environments (e.g., alkaline, salt, acid, and water solutions). They observed that fibers exhibited relatively high resistance to corrosion from salt and water, moderate resistance to corrosion from acid, and severe degradation in an alkaline solution. The tensile strength of epoxy decreased after exposure to the water and acid solutions but had little or no degradation after exposure to the alkaline and salt solutions[45]. Uthaman et al. found that CFRP composites are vulnerable to hydrochloric acid, and the SEM results showed the degradation of polymer matrix[46]. Guo et al. reported that higher

alkali content degrades not only the resin of FRPs, such as CFRP, GFRP, and BFRP but also attacks fibers, thereby accelerating the damage of the fiber-matrix interface[47]. These studies indicate that the resistance of fibers and epoxy in the same corrosive environment is different and that these materials can sometimes complement each other.

Synergistic aging. Studies on synergistic aging under multiple degradation conditions have also been reported[48–50]. One study showed that water can remove polymer microparticles formed by ultraviolet aging, exposing the undamaged material to more ultraviolet light and accelerating the aging process[50]. However, the factors that influence FRP composites depend on the service environment, including temperature, ultraviolet radiation, humidity, seawater, and corrosive action, among others. These factors involve thermodynamic, mechanical, chemical, and multifield coupling problems. Thus, these studies are insufficient and cannot provide a quantitative explanation. Further exploration of the microscopic mechanism of degradation caused by multifield coupling is necessary.

Accelerated method for durability testing

Achieving a larger period analysis of material properties through short-term experiments, i.e., using months or years of experiments to predict the service life of FRP composites or the mechanical properties after decades or more, is also a key challenge in durability research. Zhurkov conducted systematic measurements of the lifetime of 50 materials (metals and polymers) through experiments and found that the rupture lifetime τ_L conforms to the following kinetic relation[51]:

$$\tau_L = \tau_0 \exp\left(\frac{U_0 - \lambda\sigma}{k_B T}\right) \quad (1)$$

where τ_0 is the reciprocal of the natural oscillation frequency, U_0 is the binding energy at the atomic scale, λ represents the materials constants, and σ is the tensile stress. It is worth noting these were a series of macro experiments. The Arrhenius equation $k = k_0\exp(-E_a/k_BT)$, which gives the dependence of the rate constant k of a chemical reaction on a pre-exponential factor k_0, the absolute temperature T, and the activation energy E_a, is widely adopted to study the long-term durability of various materials[52,53]. To accelerate the testing process, a temperature-based accelerated method was proposed as follows:

$$\ln\left(\frac{1}{k}\right) = \frac{E_a}{k_B} - \ln k_0 \quad (2)$$

As shown in Eq. (2), the logarithm of time $\ln(1/k)$ required for a material property to reach a given value is a linear function of $1/T$, with the slope of E_a/k_BT. However, this method approximates the reaction rate to the degradation rate and requires that the activation energy E_a cannot change with temperature T. To avoid changes in the degradation mechanism, Wang et al. limited their test temperature to not exceed 60 °C[52]. Nevertheless, the actual situation may be more complex due to the heterogeneity of materials, nonuniform structure, multifield coupling, and phase changes. For example, determining the upper limit of temperature under different conditions is essential to ensure the validity of the experiment. Furthermore, understanding the relationship between this upper limit temperature and the T_g is crucial. As such, studying the microscopic degradation mechanism of FRP composites under different conditions is an urgent need.

Interfaces of FRP composites

Fiber-matrix interfaces. The fiber-matrix interfaces play an important role in the transfer of forces among the fibers and the matrix[54]. Existing studies indicate that the deterioration of interfaces can have significant effects on the mechanical properties of FRP composites[55–57]. Therefore, increasing interfacial bonding is crucial for the application of FRP composites.

In many commercial FRP composites, chemical bonding between the fibers and the matrix is usually achieved by treating the fiber surface with a sizing layer (e.g., silane coupling agent), and thus improves the interfacial adhesion[58–60], as shown in Fig. 3a–d. For GFRP composites, the graphene oxide (GO) coating enhances the shear strength of the fiber-matrix interface by creating functional groups that chemically bond with the epoxy matrix[61]. AFM observation of CFRP composites reveals that treating the fiber surface can increase the interface thickness from nanometers to hundreds of nanometers[62], as shown in Fig. 3e, f. This finding suggests that an interface with a thickness of several tens of nanometers and a gradient modulus can effectively reduce stress concentrations and transfer stress[15]. Regardless of whether the coating is carried out using GO, silane, or other sizing agents on the fiber surface, the primary aim of the coating is to enhance the bonding between the fiber and the matrix by forming thicker interphase with a gradient through surface modification.

Induced surface/interface problems in service. Furthermore, when FRP composites deteriorate in service environments, they can encounter surface/interface issues, such as fiber-matrix delamination, crack propagation, void formation/evolution, and liquid diffusion, as illustrated in Fig. 3g. An interface could have a real thickness from several atom layers to the millimeter level. As a two-phase transition region, the properties of an interface differ from those of each phase and present a continuous gradient in the direction perpendicular to the interface, as shown in Fig. 3h. Therefore, it is necessary to introduce some physical models of interface/surface for reference.

Physical models in dealing with interfacial problems and interactions at different scales

Interface/surface models at the continuum scale. There are two typical models for dealing with interface problems, namely, the Gibbs model[63] and Cahn-Hilliard model[64], as shown in Fig. 3i, j. The interface model is not only used for the interface between the fiber and matrix, but also for the diffusion or absorption of liquid, void evolution, or crack propagation of the FRP composites.

Since the actual interface has no clear boundaries, Gibbs introduced a mathematical interface without thickness, as shown in Fig. 3i. The two sides of the interface are regarded as two uniform phases, and the excess values of the physical properties generated at the interface are taken as the characteristics of the interface. The excess free energy (or interfacial energy) $\gamma_{f/m}$ of the interface can be defined as:

$$\gamma_{f/m} = \int_{-\infty}^{+\infty} F_{f/m}(x)\mathrm{d}x \quad (3)$$

where $F_{f/m}(x)$ is the free energy function. Therefore, the fiber-matrix interface can be represented by a zero-thickness Gibbs interface with interfacial energy (or adhesion energy) of $\gamma_{f/m}$. The interfacial energy can be directly calculated using MD simulation by separating the matrix from the fiber.

The interface model with diffused thickness is shown in Fig. 3j, and it can be described by the Cahn-Hilliard equation[64] as follow:

$$\frac{\partial c}{\partial t} = M\frac{\partial^2 f(c)}{\partial c^2}\nabla^2 c - 2M\chi\nabla^4 c \quad (4)$$

where $f(c)$ is the free energy density of composition c, M is the mobility, and $-M\chi$ is the correction factor for incipient surface[65].

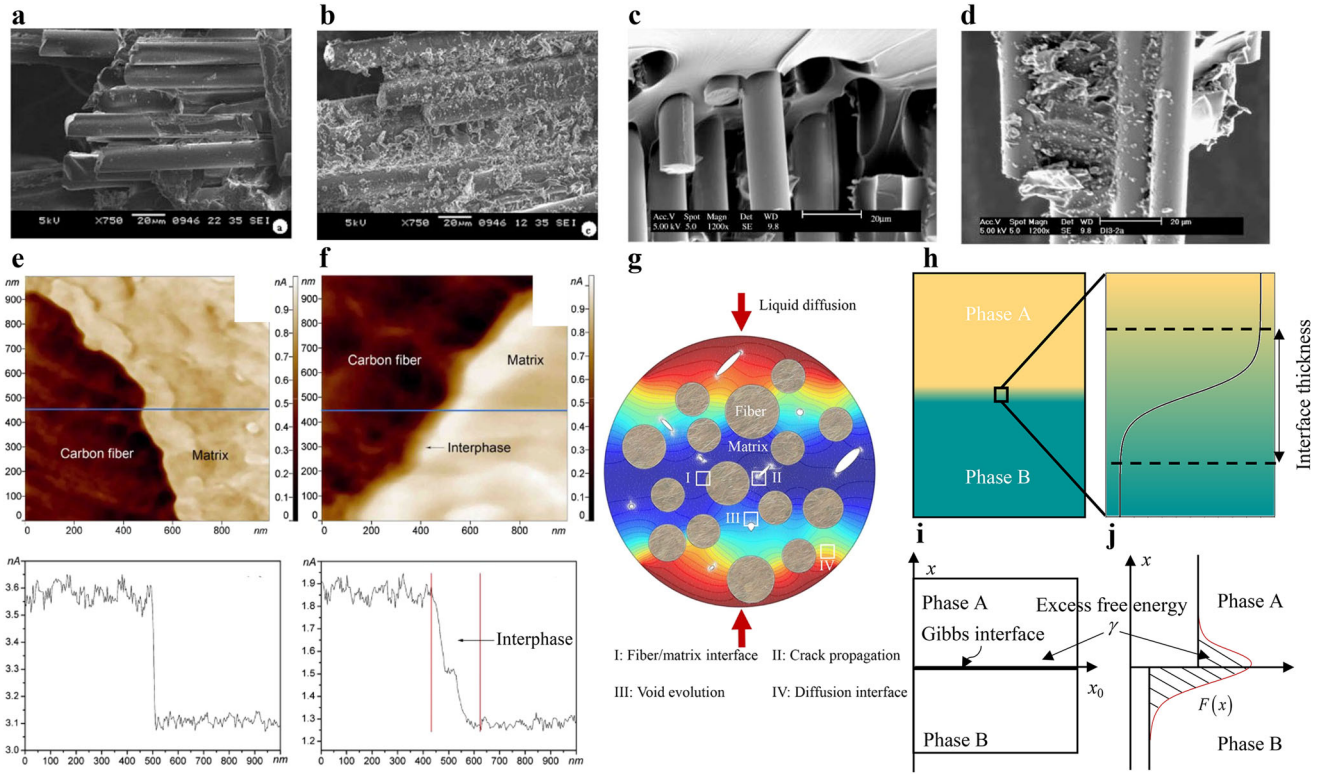

Fig. 3 Microstructure of FRP composites and interface models. SEM micrographs of the breakage region of the composites: **a** heat-cleaned GFRP, **b** 0.3% c-GPS-treated GFRP. Reprinted with permission from ref. [60]. (Copyright 2008 John Wiley and Sons). SEM images of the breakage region for different specimens that were tensile tested: **c** without coating, **d** surface coating by silane. Reprinted with permission from ref. [58]. (Copyright 2002 Elsevier). Modulus testing results of interfacial phase: **e** AFM force modulation image and section analysis of the interfacial phase in untreated carbon fiber composites; **f** AFM force modulation image and section analysis of the interfacial phase in POSS and CNT grafted carbon fiber composites. Reprinted with permission from ref. [62]. (Copyright 2015 Elsevier). **g** Schematic of four typical interfaces in FRP composite. **h** Schematic of phases A/B interface and distribution of free energy in the interface. **i** Gibbs interface model. **j** Cahn-Hilliard diffuse interface model.

Compared with Fick's second law $\partial c/\partial t = D\nabla^2 c$, the Cahn-Hilliard equation more clearly illustrates that the chemical potential, not the concentration, determines the diffusion direction. For example, $\partial^2 f / \partial^2 c < 0$ corresponds to negative diffusion, which means diffusion from low to high concentration. Phase separation processes, such as spinodal decomposition and homogeneous nucleation, are typical negative diffusion phenomena. Chemically induced phase separation was observed in the curing process[66]. Phase separation has also been used to prepare a porous epoxy monolith[67]. Void formation and transport were also observed in liquid composite molding processes[68]. Thus, the Cahn-Hilliard equation may help to understand the formation mechanism of pores/voids in the manufacturing or service of FRP composites.

The Cahn-Hilliard equation has applications in different research systems, such as solid solutions[65] and nanoscale self-assemblies[69]. Its specific form mainly depends on the interfacial free energy functional of the problem being studied[65]. In the FRP system, the interface between fiber and matrix, matrix (or fiber) and fluid, or matrix and concrete is very complex. Determining the corresponding interfacial free energy functional of FRP composites in different environments, especially under multifield coupling, is a key step in understanding their performance from the theoretical mechanism. The phase field method based on the Cahn-Hilliard equation is commonly used to predict the evolution of complex microstructures[70] and provides potential ideas for studying the diffusion of liquid, the evolution of fiber-matrix interface, void evolution, and crack propagation in FRP systems at the mesoscale, thereby playing an important role in understanding their deterioration processes.

Solid-liquid interactions in FRP composites at the nanoscale and mesoscale. For materials with small pores, voids, or gaps in a liquid environment, capillary action and disjoining pressures are very important concepts in the interaction between fluids and solids at the nanoscale and mesoscale. During production, filling the fiber gaps with liquid resin inevitably leads to voids (see Fig. 4a, b). Epoxy curing with different solvent concentrations also creates voids (see Fig. 4b, c). These processes are related to capillary action. Experimental studies indicate that the capillary action can draw moisture through the interface void of composites[71,72], making the capillary action of FRP composites in a humid/solution environment a key factor that may cause degradation.

Moreover, the liquid penetrating the interface may produce a disjoining pressure, which can rupture the bond and increase defects in the joint, leading to a reduction in its strength[73]. When studying the degradation of FRP/concrete bonding systems, it was found that the hindered adsorbed water generated a substantial disjoining pressure at the interface of the contacting cement pastes. Disjoining pressure is believed to increase stress at the tip of the microcracks, thereby hastening earlier crack propagation under external loads[74,75].

Capillary action is the flow of liquid in a narrow space without external field forces as shown in Fig. 4e. It occurs due to intermolecular forces between the liquid and the surrounding solid surface[76]. If the diameter of the narrow space is small enough, then the surface tension and the adhesion between the liquid and the solid work together to push the liquid. This is the embodiment of the Laplace pressure[77] $\Delta P = -\gamma_{lv}\,\nabla \cdot \boldsymbol{N}_s$ in the

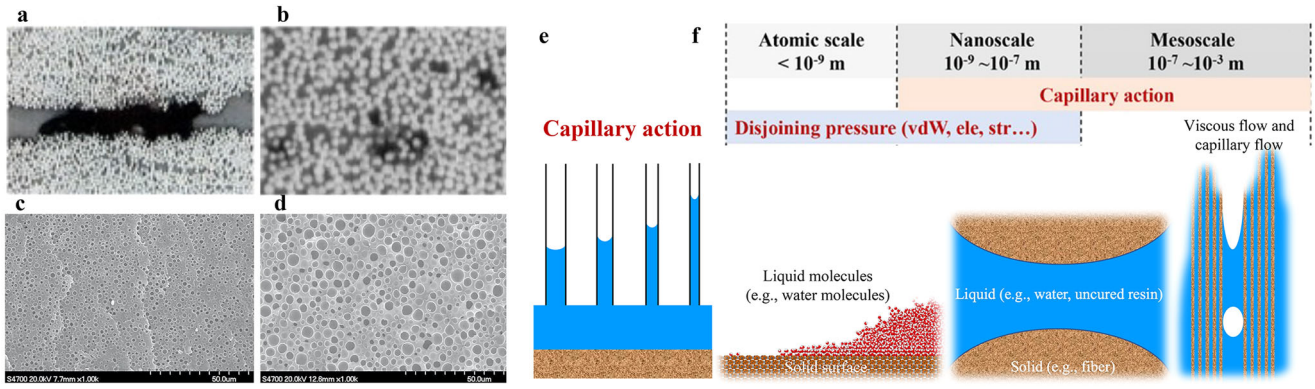

Fig. 4 Voids/pores in composites and capillary action. Void formation in liquid composite molding processes: **a** Image of the void between tows in a resin transfer molding part; **b** Image of voids inside the tow in a resin transfer molding part. Reprinted with permission from ref. [7]. (Copyright 2011 Elsevier). SEM images of porous epoxy monoliths after curing, with different solvent concentrations: **c** 30 wt%, and **d** 40 wt%. Reprinted with permission from ref. [67]. (Copyright 2009 Elsevier). **e** A schematic of the capillary phenomenon. **f** The scope of scales applicable to capillary action and disjoining pressure[80].

capillary, where γ_{lv} is the surface tension between liquid and vapor, $\boldsymbol{N}_s$ is the unit normal vector oriented outward from the surface of the liquid.

In capillary action, when the thickness h of the liquid film is below the mesoscale ($<10^{-7}$ m), the disjoining pressure becomes prominent. The disjoining pressure $\Pi(h)$ generally comes from van der Waals forces Π_{vdw}, electrostatic forces Π_{ele}, and structural forces Π_{str}[78]. For the nanoscale, the capillary force and disjoining pressure work together $p = p_{capillary} + \Pi(h)$; for the atomic scale ($<10^{-9}$ m), the disjoining pressure is mainly considered[79,80], as shown in Fig. 4f.

Interactions and destruction modes of FRP composites at atomic scale. At atomic scale, the intermolecular forces mainly include nonbonding interactions (i.e., van der Waals forces and hydrogen bonds), which are also the source of the adhesion between the fiber and the matrix. If the surface of the fiber is treated with a special coating, then a stronger chemical bond can be formed at the interface region[61]. Three typical modes of destruction in FRP composites are shown in Fig. 5a–e. In the case of fiber fracture, both the covalent bond and van der Waals interaction are disrupted (as depicted in Fig. 5a). Matrix fracture (see Fig. 5b) results in the breakage of covalent bonds, van der Waals interactions, and hydrogen bonds. The failure of the fiber-matrix interface primarily involves the disruption of van der Waals interactions, while the presence of a hydroxylated surface of the fiber can additionally result in the rupture of hydrogen bonds (see Fig. 5d, f). Furthermore, if the fiber surface has been treated with a specialized coating (e.g., GO, silane), it will also break the covalent bond (see Fig. 5c, g). In the case of debonding at a clean carbon fiber-matrix interface, only the van der Waals interaction is disrupted (see Fig. 5h).

Van der Waals force, hydrogen bond, and covalent bond at the interface. The van der Waals force constitutes a weak molecular interaction that encompasses an orientation force (present solely between polar molecules), an induction force (present between polar and nonpolar molecules), and a dispersion force (present between all molecules).

The hydrogen bond arises from a force between permanent dipoles (X-H Y), typically involving more electronegative atoms (X, Y) such as O, N, C, and F. Fig. 5i shows the hydrogen bonds formed between water molecules and polymer chains, while Fig. 5j illustrates the common hydrogen bonds in formed between polymer chains.

Table 1 General characteristics of nonbonding interactions and covalent bonds.

Type of force	Strength (kcal/mol)	Distance (nm)
Van der Waals	< 1	0.3–0.6
Hydrogen Bonds	1 ~ 40	~ 0.3
Covalent Bonds	> 40	0.074–0.267

Techniques to enhance the interface strength between the fiber and matrix include surface physical treatment to increase roughness and surface chemical modification to form additional hydrogen bonds or even covalent bonds. For example, the application of a silane coupling agent to the fiber surface results in stronger bonding between the fiber and matrix via the formation of covalent bonds with silane, as shown in Fig. 5e, g.

Nevertheless, the formation of covalent bonds necessitates specific chemical conditions (e.g., reaction sites), and the number of hydrogen bonds is generally fewer than van der Waals interactions. Even though the van der Waals force is weaker than hydrogen bonds and covalent bonds, as demonstrated in Table 1, it still plays a dominant role in numerous surface interactions (e.g., adhesion[81,82], adsorption[83,84], etc.) due to its ubiquity. Specifically, when the surface is rough, the specific surface area is significantly increased, resulting in stronger adhesion.

Bridging length and time scales in durability studies of FRP composites

This section aims to introduce multiscale simulation methods (see Fig. 1), and some fundamental theories and concepts (e.g., kinetic theories, Hamaker constant) that may be used in durability studies of FRP composites.

Atomic scale methods. At the atomic scale, quantum chemistry simulation can be used to address issues involving charge transfer, such as cross-linking reactions, degradation, and chemical bond formation or breaking. First principles based on multi-electron systems and density functional theory (DFT) based on space charge density are the primary calculation methods. These methods can also provide potential parameters for molecular simulations. Due to the large number of calculations required to account for the movement of electrons, hybrid quantum mechanical/molecular mechanical (QM/MM) methods and

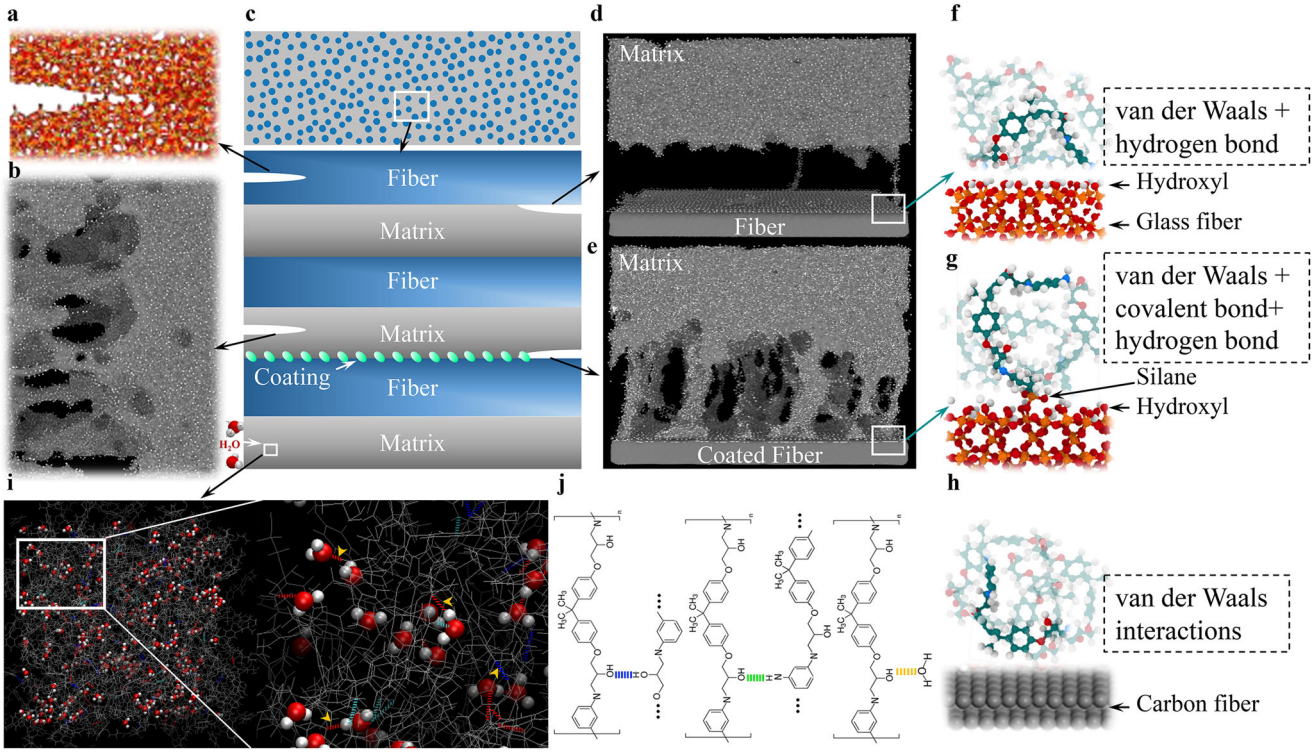

Fig. 5 Typical modes of destruction in FRP composites and microscopic damage mechanisms. a–e Typical modes of destruction in FRP composites: Fracture in fiber (**a**) and matrix (**b**); **c** Schematic diagram at the mesoscale; Debonding of uncoated fiber-matrix interface (**d**) and coated fiber-matrix interface (**e**). **f** Van der Waals interaction and hydrogen bond between the polymer and the hydroxylated surface of silica. **g** Silane coupling agent bonds fiber and matrix by forming covalent bonds. **h** Van der Waals interaction between polymer chain and carbon fiber. **i** Water molecules enter the matrix; **j** Hydrogen bond between the hydroxyl groups of the polymer chain O-H O (blue); Hydrogen bond between the hydroxyl and amino O-H N (green); Hydrogen bond between the water and hydroxyl of the polymer chain O-H O (yellow).

AIMD methods have been developed to maintain accuracy and improve efficiency. AIMD methods have been employed to examine hydrogen bonding, ionic bonding, and van der Waals interactions between polymers and cement[85], and can be utilized for durability studies of FRPs under environmental conditions.

Nanoscale methods and associated analytical models. At the nanoscale, MD simulations, which are based on the potential function and force field parameters, are widely used to determine the thermal and mechanical properties of the system through statistical averaging. For example, T_g can be determined by simulating the density change with temperature[22,38]. The adhesion energy E_{adhesive} between the matrix and the fiber can be obtained through interfacial separation: $E_{adhesive} = E_{fiber} + E_{matrix} - E_{matrix@fiber}$.

The classical force field cannot handle the formation and breakage of chemical bonds; therefore, reactive force fields, such as REBO[86] and ReaxFF[87,88] are required to simulate chemical reactions. These force field parameters can be obtained through advanced parameterization methods[89] based on DFT data, as well as through the use of machine learning (ML) to obtain the ML force field[90]. All of these approaches will facilitate the application of MD methods in a wider range of materials and engineering fields, and will also benefit the durability research of FRP.

Kinetic theories. Several kinetic theories are commonly used to analyze MD simulation results. The modified Bell model is widely used in the analysis of polymer dynamic peeling and shear/creep on the fiber surface[91,92]:

$$v = \omega_0 x_b \exp\left(-\frac{E_b - f \cdot x_b}{k_B T}\right), \tag{5}$$

where v is the pulling speed, and f is the pulling force. By plotting f against $\ln v$, the adhesion energy E_b of peeling/shear/creep and the distance between the equilibrated state and the transition state x_b can be quantified. The fundamental frequency ω_0 is the conversion factor $k_B T/h|_{T=300K} \sim 10^{13}$ Hz of the transition state product in the transition state theory (TST)[93]. Similarly, when studying the wetting behavior in FRP systems, molecular kinetic theory (MKT) can also be used. This theory is also established based on statistical theory[80,94,95]: $j = (k_B T/h)\exp(-\Delta G/k_B T)$. The frequency of molecular jumping j is a function of activation free energy ΔG. The modified Bell model, MKT, and TST are compared in Fig. 6.

Diffusion and relaxation. The diffusion coefficient D can also be obtained from MD simulation by analyzing the mean squared displacement (MSD) of the molecule:

$$D = \frac{1}{6}\frac{d}{dt}\left\langle \left| \boldsymbol{r}_t - \boldsymbol{r}_0 \right|^2 \right\rangle, \tag{6}$$

where $\boldsymbol{r}_t$ and $\boldsymbol{r}_0$ are the position vectors of particles at time t and initial time respectively. The diffusion coefficient can be used in Fick's law: $\boldsymbol{J} = -D\nabla c$. Many experimental studies of moisture diffusion in epoxy or FRP composites have shown that the initial diffusion conforms to Fick's law, and as the temperature or saturation increases, the diffusion exhibits non-Fickian behavior[96,97]. Berens et al. proposed a more general model for polymeric materials $M_t = M_{t,F} + M_{t,R}$, which consists of Fickian diffusion $M_{t,F}$ and polymeric relaxation $M_{t,R}$[97,98]. When considering the coupling effect of relaxation time τ on flux $\boldsymbol{J}(r,t+\tau) = -D\nabla c(r,t)$, the modified Fick's second law can be obtained

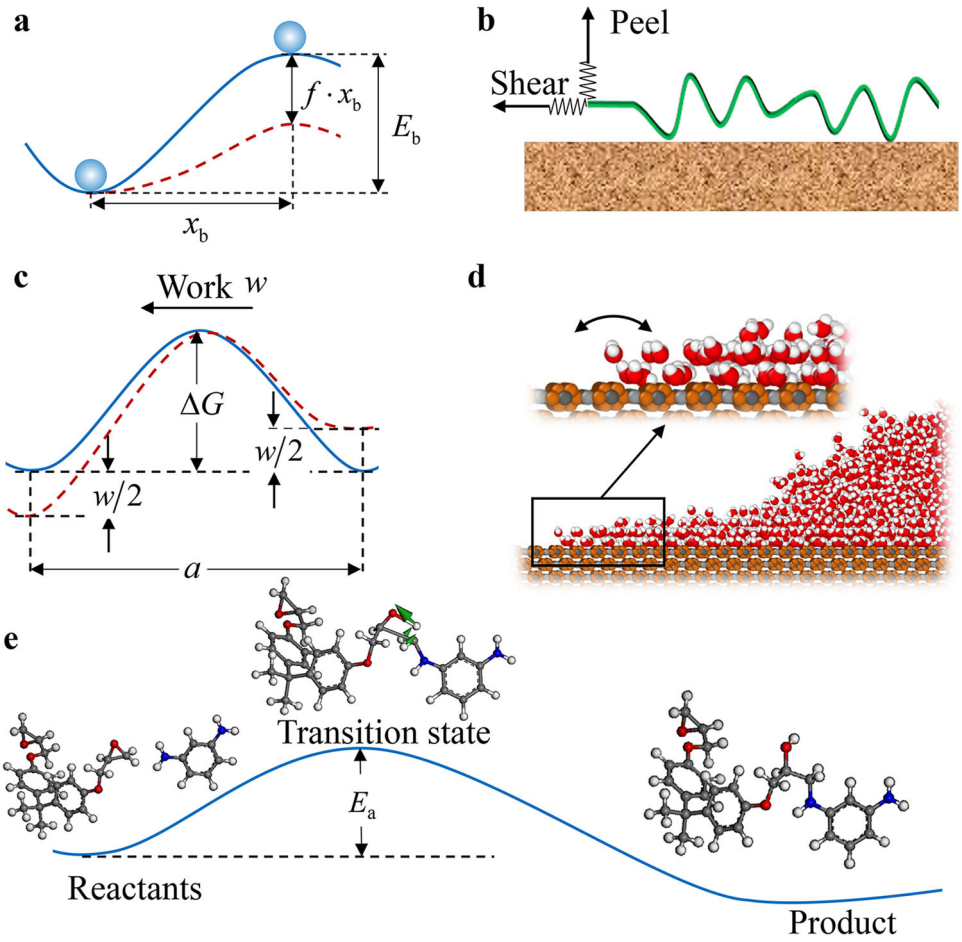

Fig. 6 Kinetic theories that may be used in the study. a Modified Bell model: The external force work $f \cdot x_b$ reduces the energy barrier E_b for bond breaking. The blue circle represents the state of the bond, such as the equilibrium state and transition state. **b** Two types of forces of polymer chain on the substrate surface, i.e., peeling and shearing. **c** The Molecular kinetic theory (MKT) describes the interaction between liquid and solid surfaces. The diagram illustrates the transition of the system from a non-equilibrium state (red dashed line) to an equilibrium state (blue line) under the influence of driving work w. **d** Schematic of the wetting process of water molecules on a solid surface. **e** Transition state search diagram: Along the reaction coordinate, from reactants (such as epoxy resin and curing agent) to the transition state, and finally forming the crosslinked product. It allows for obtaining the reaction energy barrier E_a, providing information about the chemical reaction kinetics.

as follows[99]:

$$\frac{\partial c}{\partial t} + \tau \frac{\partial^2 c}{\partial t^2} = D\nabla^2 c \quad (7)$$

Considering the lag of flux τ_1 and concentration τ_2 simultaneously, a dual-phase-lag diffusion model was proposed[100] $\boldsymbol{J}(r,t+\tau_1) = -D\nabla c(r,t+\tau_2)$. In addition to the relaxation time in diffusion, there are many models to describe the relaxation in these studies of the physical aging of polymers[101] (e.g., Moynihan model, KAHR model, and coupling model). Hence, accurately determining the relaxation time is a crucial step in the study of both liquid diffusion and physical aging of polymer. MD simulation provides a potential way to determine the relaxation time accurately at the nano/microscale.

Mesoscale methods. At the mesoscale, the CG method has significantly increased the scales of molecular simulation by reducing the degrees of freedom. Molecules or functional groups are represented by pseudoatoms approximating groups of atoms. There are two typical CG simulation methods: CG MD and CG dissipative particle dynamics (DPD). The interaction parameters of pseudoatoms or beads can be derived from all-atom MD simulations.

Hamaker constant is an important parameter bridging the nanoscale and mesoscale, which can be obtained through MD simulation or experiment. The van der Waals force F_{vdw} between the two phases can be predicted by the Hamaker constant, i.e., $F_{vdw}=-A/(6\pi D^3)$. The Hamaker constant $A = \pi^2 C_{vdw}\rho_1\rho_2$ is related to the atom pair potential coefficient (C_{vdw}) and atom number density (ρ_1, ρ_2) in the two phases. Through AFM measurement, the Hamaker constants of organic small molecules on the carbon fiber surface are typically around $4 \sim 5 \times 10^{-20}$ J[102], which are almost an order of magnitude lower than that of modified carbon fibers ($\sim 2.8 \times 10^{-19}$ J)[103].

The phase field method, a powerful tool for multifield coupling simulation at the mesoscale, can be used to predict the evolution of complex microstructures without explicitly tracking the positions of interfaces. The parameters involved in the phase field simulation, such as permeability k and mobility M, can be obtained from MD simulations[104] or experiments[71,105–108]. With the fundamental thermodynamic and kinetic properties, the phase field method is capable of predicting the evolution of mesoscale morphological and microstructure in materials[70]. It provides potential solutions for studying the formation of voids in FRP systems and their evolution during long service.

Table 2 Comparison of simulation methods: DFT, ReaxFF MD, Classical/CG MD.

Method	DFT	ReaxFF MD	Classical/CG MD
Scale (m)	10^{-10}~10^{-9}	10^{-9}~10^{-7}	10^{-9}~10^{-6}
Advantages	High precision	Coupled mechanical and chemical processes	More force fields; Simulate larger and complex systems
Disadvantages	Small system (Hundreds of atoms)	Slower than classical MD; Force field parameters need to be developed	Cannot simulate chemical reactions
Features	Chemical properties; Reaction mechanism; Provide parameters for MD	Reaction process; Bond breaking process; Thermodynamic properties; Mechanical properties	Dynamics process; Thermodynamic properties; Mechanical properties
Examples	Activation energy of cross-linking reaction; Potential parameters; Chemical bond parameters, etc.	Corrosion (acid, alkali); Chemical deterioration; Debonding process (coupling agent), etc.	Diffusion of water and ions in FRP; Physical deterioration; Debonding process, etc.

Methods in continuum mechanics. At the macroscale, FEM simulations and macro experiments are widely used in the study of the mechanical properties of structural materials. To accurately represent the damage processes and failure mechanisms of FRPs, such as crack growth and fiber-matrix interface debonding, small elements are required in FEM simulations. Mesoscale finite element (Meso-FE) models of composites are a robust approach for homogenizing mechanical properties, examining stress-strain fields within cells, identifying damage initiation conditions and locations, and simulating damage progression and the associated degradation of composite homogenized mechanical properties[109]. Koloor et al.[110] introduced a damage model and integrated it with the FE model-based construction to evaluate the elastic-to-failure behavior of CFRP and GFRP composite laminates manufactured via different methods. Ullah et al.[111] devised a three-dimensional multiscale computational homogenization framework to predict the nonlinear meso-/macroscopic mechanical behavior of FRP composites.

The distribution of fiber orientations is critical to the mechanical performance of FRP composites, and the distribution functions can serve as accurate microstructural descriptors of the axisymmetric fiber orientation within a specific volume of a fiber-reinforced composite[112,113]. Fiber orientation tensors serve as a measure of the average fiber orientations within a microstructure[113,114]. The anisotropic behavior of the material is a result of the reorientation effect of the fibers during the extrusion process. To gain insight into the relationship between fiber orientation and geometric parameters, a fiber orientation model was incorporated into a particle finite element method (PFEM) based framework for simulating the process[115].

In a cross-scale study, interfacial parameters generated by MD simulation were used in the FEM simulation by converting them to parameters of the cohesive zone model (CZM)[116]. The simulation results of ultimate bond strength and structural behavior show agreement with the experimental results. However, it should be noted that the macro structures or materials often have defects and heterogeneity, and thus are more complex than the microscopic ones. Therefore, the validity of the parameters needs to be considered when the microscopic parameters are used in the macro analysis.

The main methods involved in a multiscale simulation are introduced above. From atomic scale to mesoscale, the atomistic/molecular simulation methods include DFT, ReaxFF MD, classical MD, and CG MD. Table 2 provides an overview of the advantages, disadvantages, and features of these methods. The table also presents examples of simulation methods that correspond to typical processes in FRP composite research, allowing for a more targeted selection of simulation methods.

Atomic- and molecular-scale simulations of FRP composites

Considering MD simulation is a bridge between quantum chemistry and continuum mechanics in multiscale modeling. This section mainly reviews the role and progress of MD simulations in the study of the mechanical properties and durability of FRP composites.

Cross-linking simulations of polymers. Cross-linking includes physical and chemical cross-linking. The former is linked by weak interactions, such as ion bonds and hydrogen bonds[117]. The latter is the process of forming covalent bonds between polymer chains. In the manufacturing of FRP composite, curing is a chemical process that involves the cross-linking of polymer chains. It should be noted that in this context, the term "cross-linking" specifically refers to chemical cross-linking.

Polymeric materials with a high degree of cross-linking generally exhibit good mechanical properties, which are critical for ensuring the structural integrity of polymeric composites. MD simulations have been widely used to investigate the morphology, structure, and mechanical properties of cross-linking networks in polymeric materials[21,22,118–123]. The simulation process typically involves the preparation of unlinked molecular monomers, initialization of the MD simulation, MD cross-linking simulation, and relaxation of the system to equilibrium. To improve the efficiency of the cross-linking simulation, different algorithms and conditions are often used depending on the reaction system. For instance, the bond formation may occur only when the distance between reactive atoms falls within a certain reaction cut-off[119,124–127]. Wu et al.[119] reported an algorithm where the conversion of diglycidyl ether bisphenol A (DGEBA) and isophorone diamine (IPD) reached 93.7%. Varshney et al.[127] proposed a multistep relaxation procedure for relaxing the monomers during cross-linking, which has shown effectiveness in constructing larger cross-linking networks. Furthermore, Sharp et al.[122] investigated the effects of water on the cross-linking of epoxy resins using MD simulations and found that water increased molecular diffusion, leading to an increase in the curing rate at the initial stage of cross-linking.

It is worth noting that most cross-linking simulation methods rely solely on the distance between the atoms/particles of interest to determine bond formation, without considering the effects of geometry and steric hindrance. To simulate more realistic chemical reactions, the development of reactive force fields (e.g., REBO[86] and ReaxFF[87,88]) is required. However, using a reactive force field to perform cross-linking simulations can be inefficient. To address this issue, van Duin et al.[128] proposed a new method developed within the framework of ReaxFF that accelerates the cross-linking reaction by providing sufficient

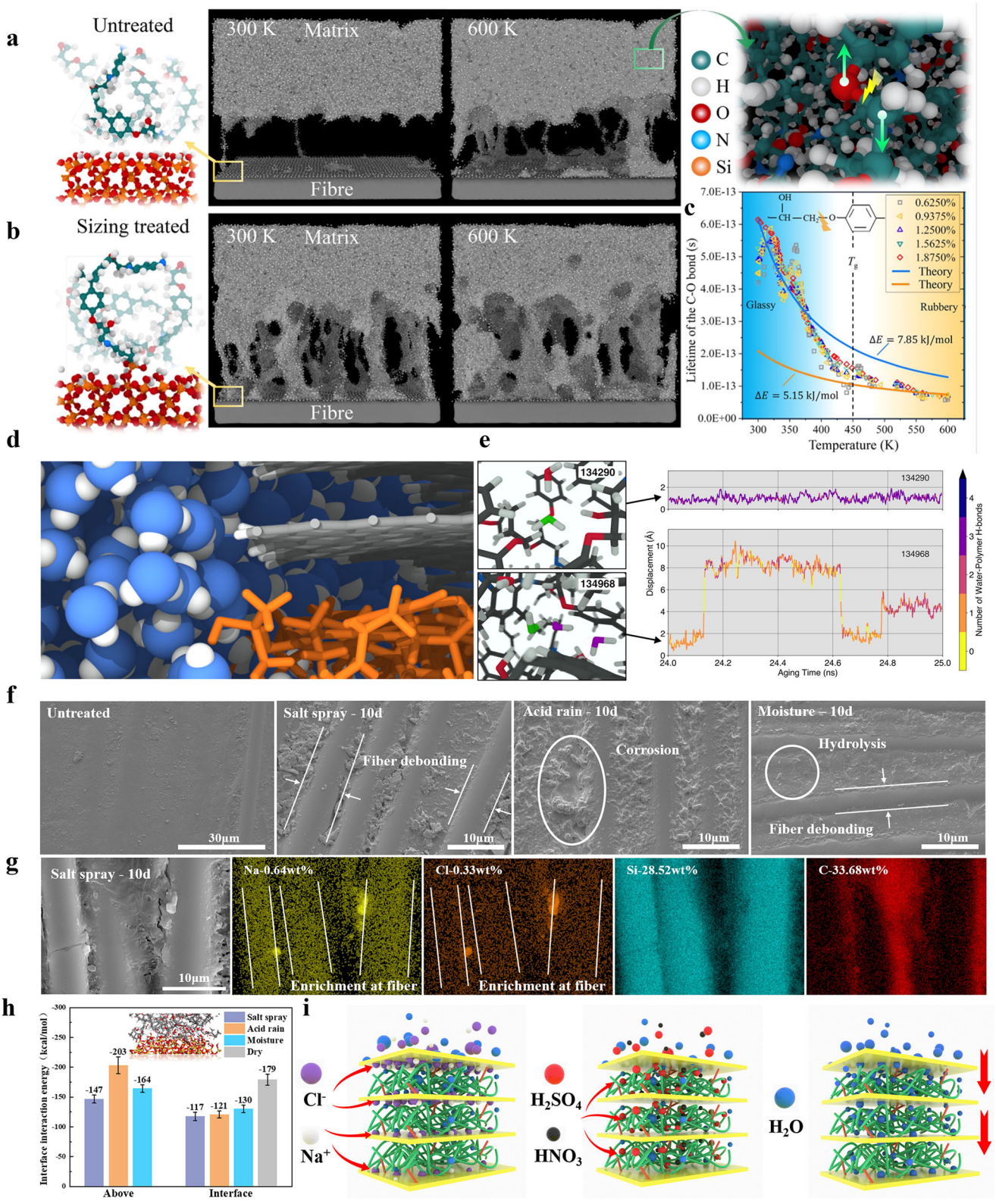

Fig. 7 Typical studies on the properties of fiber-polymer interfaces using MD and experimental methods. The properties and deterioration mechanism of fiber-polymer interfaces (i.e., untreated fiber-epoxy interface (**a**) and sizing-treated fiber-epoxy interface (**b**)) under coupled thermal-mechanical actions; **c** the average lifetime of the C-O bonds during initial debonding as a function of temperature. Reprinted with permission from ref. [22]. (Copyright 2022 Elsevier). **d** Carbon fiber-epoxy interface exposed to liquid water; **e** displacement of two exemplar water molecules of hygrothermal aging. Reprinted with permission from ref. [153]. (Copyright 2020 American Chemical Society). **f** SEM images of the surface morphology of the samples aged for 10 d under the salt spray, acid rain, and moisture; **g** energy dispersive spectroscopy (EDS) of sample aged for 10 d under salt spray; **h** Interfacial energy obtained by MD simulations; **i** Schematic diagram of liquid diffusion. Reprinted with permission from ref. [152]. (Copyright 2022 Elsevier).

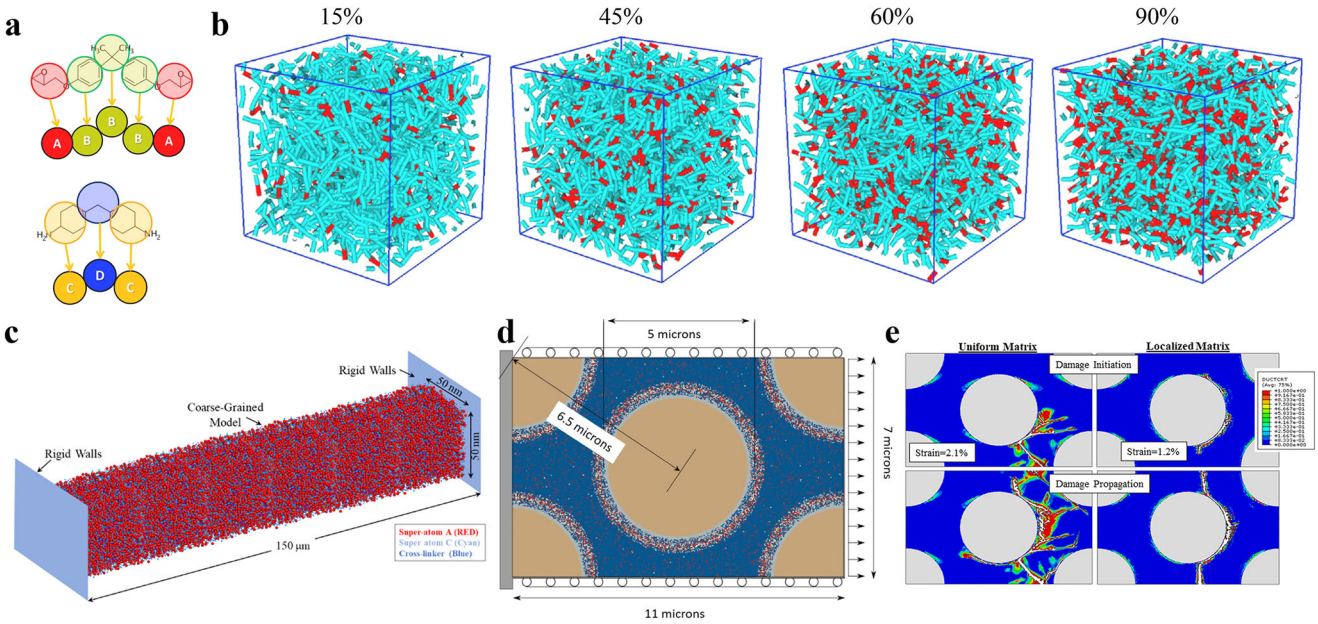

Fig. 8 CG modeling and multiscale simulations. a CG particles for DGEBA and PACM; **b** CG models of epoxy (DGEBA-PACM) with cured conversions of 15%, 45%, 60%, and 90%. Reprinted with permission from ref. [161]. (Copyright 2022 Elsevier). **c** A CG-model of epoxy matrix confined between two rigid walls; **d** FEM model of composite combined with the CG MD simulations; **e** Contours of the ductile damage initiation criterion for uniform matrix model and localized matrix model at two different strain levels. Reprinted with permission from ref. [163]. (Copyright 2020 American Chemical Society).

energy to overcome reaction barriers, based on the distance and orientation of the reactants. If a more detailed understanding of the cross-linking process is required, beyond simply constructing a cross-linked model, then using a reaction force field to simulate the cross-linking is a better option.

Microscopic model and mechanical studies of FRP composites. FRP composites consist of fibers (e.g., carbon fibers, glass fibers, basalt fibers, or aramid fibers) and matrix (e.g., polymeric resin) bonded through interfaces. In addition to the previously discussed resin modeling, the interfacial model and properties are also related to the type of fiber. The common model for carbon fiber is graphite/graphene[129–133], while silica is commonly used to model glass fiber[92]. Due to the complicated composition of aramid or basalt fibers, only a few related studies have suggested that aramid fiber can be modeled by p-phenylene terephthalamide (PPTA) filaments[134].

Three typical failure mechanisms may exist in FRP systems, i.e., interface debonding, matrix failure, and fiber breakage[135], as shown in Fig. 5c. The strength of the fiber is the largest among the three components[136,137], and the strength of the interface and the matrix depends on the specific material and processing technology. Surface treatment of the fiber can enhance the bonding between the fiber and the matrix, potentially leading to failure in the matrix rather than at the interface. Therefore, the study of the mechanical properties of the interfacial phase, as shown in Fig. 5d, e, becomes crucial. MD simulations can capture the details of the interfacial phase evolution[22] and obtain micromechanisms of macroscopic properties. This technique enables researchers to gain new insights into the mechanical properties at the nanoscale and contribute to the design of FRP composites.

Zhang et al.[138] built an interface model consisting of glass fiber, a sizing layer, and a polypropylene (PP) matrix and performed tensile simulations on the interface model using a CVFF forcefield. Lin et al.[22] established two glass fiber-epoxy interface models to investigate the effects of fiber sizing in debonding at various temperatures using ReaxFF MD simulations. Both studies showed that for fibers treated with sizing on the surface, the fracture does not occur at the fiber surface but in the matrix. Niuchi et al.[139] simulated the effect of chemically modifying the surface of carbon fiber on the interfacial strength between carbon fiber and phenolic resin. The results show that the interfacial strength of the model with fluorinated carbon groups is lower than that of the model with only carbon atoms. Wang et al.[140] explored the effect of acid treatment time on the shear strength of the interface using MD simulations and indicated that the functional groups on carbon fibers increase the micro-mechanical interlocking effect at the interface. The Bell model has been widely used to analyze the energy barrier of interfacial deformation for understanding the creep behavior at the molecular level[141,142].

Polymeric-based composites are viscoelastic, making their time-dependent behavior one of the most critical factors in the design of FRP structural system[143]. Creep is one of the time-dependent phenomena, which reflects the relaxation of materials. Tam et al.[141,144] explored the creep behavior of the fiber-matrix interface at different loads and found a threshold stress for the onset of creep failure, which decreases in moisture conditions.

Environmental effects on the properties of FRP composites. Numerous macroscale studies have suggested that environmental factors, such as temperature[145–147], moisture[148,149], and salt environments[147,150], can decrease the adhesion in the bonded area of FRP composites. To explore the intrinsic mechanism of debonding of FRP composites, researchers have employed MD simulations to study the thermal and mechanical properties of fiber-polymer interfaces[22,138]. Lin et al.[22] found that the elastic modulus and the peak stress decrease with increasing temperature, and elucidated the mechanism of mechanical properties changing from the glassy to the rubbery state, as shown in Fig. 7a–c. Several MD studies[151,152] have shown that water and salt degrade the interfacial bonding of the fiber-polymer system by decreasing the adhesion energy. Notably, simulations by Walsh et al.[153] showed that the fiber-matrix interface is less sensitive to early water ingress and is not easily to be flooded in the early stages of water aging. They observed that water is

primarily absorbed through the matrix-water interface, and this entry pathway is facilitated by the dynamic mobility of the polymer chains at this interface (see Fig. 7d, e). Guha et al.[154] calculated the diffusion coefficient (D) from the MSD of water molecules and found that the moisture initially diffuses in the bulk and eventually accumulates at the damaged system, with absorbed moisture concentrated at the interface. Xie et al.[152] combined experiments and MD simulations to illustrate the hydrothermal aging of the fiber-epoxy interface. The simulation results indicated that NaCl tended to diffuse and accumulate at the fiber-epoxy interface, leading to serious fiber peeling. In the case of acid rain, oxidizing acid particles tended to react with the epoxy and the diffusion behavior was a layer-by-layer erosion process (see Fig. 7f–i).

MD simulations have revealed that the micromechanisms of the reduction of the adhesion energy of interfaces in moisture mainly include two aspects: first, water molecules enter the interface thus disrupting the interaction between the fiber and the matrix; second, molecules enter the epoxy and break the original H-bonds, thus degrading the structure. However, the conclusion that salt environments are more likely to cause interfacial debonding than humid environments has been explained only from a phenomenological perspective without fundamental physical insights. In addition, most MD studies in this field have focused on degradations of nonbonding interactions, which do not involve the breaking and formation of chemical bonds. Chemical degradation may be involved in actual long-term service. As such, more precise simulation methods (e.g., DFT, Ab initio MD, ReaxFF MD) could be used in future studies to address these issues.

CG modeling and multiscale simulations. In mesoscale simulations, CG modeling is often used as a multiscale method, as the interaction parameters between the beads must be determined by full-atomic molecular simulation. The length scale of the CG simulation is generally on the order of $10^{-8} \sim 10^{-7}$ m, which is at least one order of magnitude higher than the length scale used in full-atom MD simulation.

In CG models, molecules or functional groups are represented not by individual atoms but rather by pseudoatoms that approximate groups of atoms. By reducing the degrees of freedom, CG models sacrifice molecular details for the ability to study longer simulation time and larger simulation systems. CG models have been practically applied in MD simulations of polymer materials[155–157]. In CG molecular models of epoxy-based materials, several monomer units are represented by a single bead[25,158]. Many studies have successfully used CG MD simulations to investigate the mechanical properties of polymer materials[159–163]. Shoji et al.[161] developed a CG model of DGEBA-PACM epoxy that reproduces the experimental density, as shown in Fig. 8a, b. Liu et al.[25] constructed a CG DPD model, combined with the curing reaction to simulate the formation of cross-linked structures consisting of carbon fibers, sizing agents, and epoxy. The simulation results showed that the components can diffuse among each other, greatly influencing the generated network structure during the curing process. Zhang and Liew et al.[162] identified a novel mechanism called "debonding-induced crazing" using a multiscale method (i.e., CG method and full-atom MD method) that controls the transition from cavitation to crazing in polymeric composites. In addition to the multiscale method used in the CG modeling process, the free volume distributions obtained by CG MD simulations have also been successfully upscaled into FEM simulation, as a multiscale method (i.e., CG MD-informed FEM, see Fig. 8c–e), to predict the damage around the fiber-matrix interface[163].

Although the multiscale methods offer a potential way to analyze and explain phenomena across different scales, the accuracy of parameter transfer between different scales needs to be verified. The scale effect and the scope of parameter transfer must be carefully considered.

Multiscale voids in FRP composites. During the liquid composite molding process, the impregnation of fibers may not be complete, resulting in nonwetting and possibly causing voids[164]. Experimental studies have also shown that the voids in FRP composites exhibit multiscale features ranging from nanoscale[165,166] to micron scale[167]. The voids directly affect the mechanical properties of the FRP system. Tan and Martínez-Pañeda[168] developed a phase field model to predict the microscopic fracture of FRP composite and revealed that the crack paths are highly dependent on the void volume fraction. Johnston et al.[169] presented a multiscale modeling framework that combines a new molecular interphase model, consisting of voids in multiple graphene layers, for the analysis of polymeric composites. Furthermore, the diffusion of water, salt, and other particles occurs due to the existence of voids within the materials. Thomason demonstrated that void content is the key factor in the moisture absorption of GFRP composites[170]. Harper et al.[171] found that for graphite/epoxy composites with low void content, moisture follows the classical Fickian diffusion, while composites with high void content exhibit some anomalies of non-Fickian diffusion[172].

Moisture, salt ions, and other particles can enter the interior of voids through capillary forces and diffusion, leading to hygrothermal effects and deterioration. However, there are few microscopic studies on the effect of voids or pores in the matrix on the durability of FRP composites. Directly simulating the evolution of micron-scale voids using MD simulations is not practical. Nonetheless, MD simulation is a potential method to reveal the atomic- and molecular-level mechanisms of void growth and predict the properties of voids at the nanoscale, which can be used to generate input properties for multiscale modeling.

Summary and outlook

This review commences with a brief introduction to fundamental concepts in micro-/nano-mechanics and multiscale simulation methodologies employed in the investigation of FRP composites. The effects of environmental factors, such as temperature, ultraviolet radiation, humidity, seawater, and corrosion on the properties of FRP composites are reviewed, taking into account the complex interplay of thermal, mechanical, and chemical coupling phenomena. Given the intricate interface problems encountered during deterioration (e.g., diffusion, debonding, fracture, cavitation, crazing, etc.), representative interface models are introduced. To gain insights into the durability and degradation mechanisms of FRP composites at the microscale level, relevant micro/nano mechanics topics are expounded, including van der Waals interactions, hydrogen bond interactions, disjoining pressure, and capillary action. Furthermore, the acceleration technique for durability testing and its applicable conditions are delineated. MD simulations serve as a vital link between quantum chemistry and continuum mechanics within the context of multiscale methods. The review's latter portion primarily surveys the role and research status of MD simulations in the examination of mechanical properties and durability of FRP composites, encompassing ReaxFF MD simulations, classical MD simulations, and CG MD simulations. Lastly, the challenges and issues associated with multiscale void analysis in FRP composites are briefly outlined.

From the perspective of micro-/nano-mechanics, four pivotal scientific issues are identified to address the intricate problem of FRP composite durability under multiple environmental factors:

1. The complexity of interface phenomena (e.g., diffusion, debonding, fracture, cavitation, crazing, etc.) necessitates

determining the corresponding interfacial free energy functional of FRP composites in diverse environments, particularly under multifield coupling, as a crucial step towards comprehending interface evolution.
2. Capillary action and disjoining pressure represent essential concepts in nano/mesoscale interactions between fluids and solids, which are crucial for understanding the initial void/bubble formation mechanism during FRP composite production and the degradation mechanism during service in humid conditions.
3. Relaxation time is a central concern in phase diffusion and the physical aging of polymers. Accurately obtaining relaxation time for various physical behaviors is critical for understanding degradation. MD simulations offer a potential avenue for precise relaxation time determination, albeit with scale limitations, necessitating an up-scaling approach.
4. The Arrhenius equation is extensively employed to study the long-term durability of FRP composites. This method assumes that the degradation mechanism remains invariant with temperature. However, the actual scenario is more complex, with material heterogeneity, nonuniform structure, multifield coupling, and phase change posing significant challenges for the temperature acceleration method in durability testing.

In conclusion, this paper does not endeavor to provide an exhaustive review of all advancements in the field of mechanical properties and durability studies of FRP composites. Instead, it selectively covers several typical subjects within the vast domain, highlighting key concerns. The primary aim is to elucidate the role of MD simulations in FRP composite research and outline future prospects, demonstrating how micro-/nano-mechanics can contribute to the study of FRP durability.

Received: 1 December 2022; Accepted: 17 August 2023;
Published online: 30 August 2023

References

1. Aamir, M., Tolouei-Rad, M., Giasin, K. & Nosrati, A. Recent advances in drilling of carbon fiber–reinforced polymers for aerospace applications: A review. *Int. J. Adv. Manuf. Technol.* **105**, 2289–2308 (2019).
2. Teng, J., Chen, J.-F., Smith, S. T. & Lam, L. *FRP: strengthened RC structures*. (John Wiley & Sons, 2002).
3. Hollaway, L. C. & Teng, J.-G. *Strengthening and rehabilitation of civil infrastructures using fibre-reinforced polymer (FRP) composites*. (Woodhead Publishing, 2008).
4. Teng, J. G., Yu, T., Wong, Y. L. & Dong, S. L. Hybrid FRP–concrete–steel tubular columns: Concept and behavior. *Const. Build. Mater.* **21**, 846–854 (2007).
5. Yu, T. & Teng, J. G. Design of concrete-filled FRP tubular columns: provisions in the chinese technical code for infrastructure application of FRP composites. *J. Compos. Const.* **15**, 451–461 (2011).
6. Bank, L. C. *Composites for construction: structural design with FRP materials*. (John Wiley & Sons, 2006).
7. Park, C. H., Lebel, A., Saouab, A., Bréard, J. & Lee, W. I. Modeling and simulation of voids and saturation in liquid composite molding processes. *Compos. Part A-Appl. S.* **42**, 658–668 (2011). **This study investigated the influence of the global resin flow upon the void formation**.
8. Soles, C. L. & Yee, A. F. A discussion of the molecular mechanisms of moisture transport in epoxy resins. *J. Poly. Sci. Part B: Poly. Phys.* **38**, 792–802 (2000).
9. Sen, R. Developments in the durability of FRP-concrete bond. *Constr. Build. Mat.* **78**, 112–125 (2015).
10. Zhang, X. et al. Atomistic measurement and modeling of intrinsic fracture toughness of two-dimensional materials. *Proc. Nat. Acad. Sci.* **119**, e2206756119 (2022).
11. Chen, L. et al. Enhanced epoxy/silica composites mechanical properties by introducing graphene oxide to the interface. *ACS Appl. Mater. Interf.* **4**, 4398–4404 (2012).
12. Benmokrane, B., Ali, A. H., Mohamed, H. M., ElSafty, A. & Manalo, A. Laboratory assessment and durability performance of vinyl-ester, polyester, and epoxy glass-FRP bars for concrete structures. *Compos. Part B: Eng.* **114**, 163–174 (2017).
13. Mourad, A.-H. I., Abdel-Magid, B. M., El-Maaddawy, T. & Grami, M. E. Effect of seawater and warm environment on glass/epoxy and glass/polyurethane composites. *Appl. Compos. Mat.* **17**, 557–573 (2010).
14. Benmokrane, B., Elgabbas, F., Ahmed, E. A. & Cousin, P. Characterization and Comparative Durability Study of Glass/Vinylester, Basalt/Vinylester, and Basalt/Epoxy FRP bars. *J. Compos. Constr.* **19**, 04015008 (2015).
15. Zhao, F., Huang, Y., Liu, L., Bai, Y. & Xu, L. Formation of a carbon fiber/polyhedral oligomeric silsesquioxane/carbon nanotube hybrid reinforcement and its effect on the interfacial properties of carbon fiber/epoxy composites. *Carbon* **49**, 2624–2632 (2011).
16. Chen, L. et al. A design of gradient interphase reinforced by silanized graphene oxide and its effect on carbon fiber/epoxy interface. *Mater. Chem. Phys.* **145**, 186–196 (2014).
17. Wang, Z. et al. Long-term durability of basalt- and glass-fibre reinforced polymer (BFRP/GFRP) bars in seawater and sea sand concrete environment. *Constr. Build. Mater.* **139**, 467–489 (2017).
18. Czabaj, M. W., Riccio, M. L. & Whitacre, W. W. Numerical reconstruction of graphite/epoxy composite microstructure based on sub-micron resolution X-ray computed tomography. *Compos. Sci. Technol.* **105**, 174–182 (2014).
19. Tatar, J., Brenkus, N. R., Subhash, G., Taylor, C. R. & Hamilton, H. R. Characterization of adhesive interphase between epoxy and cement paste via Raman spectroscopy and mercury intrusion porosimetry. *Cem. Concr. Compos.* **88**, 187–199 (2018).
20. Zhao, Y.-P. *Nano and Mesoscopic Mechanics*. (Science Press, 2014).
21. Lin, K. & Yu, T. Debonding simulation of fibre-matrix interfaces of FRP composites with reactive force field. *Constr. Build. Mater.* **312**, 125304 (2021).
22. Lin, K. & Yu, T. On the properties and deterioration mechanism of fibre-matrix interfaces of FRP composites under coupled thermal-mechanical actions. *Compos. Part A-Appl. S.* **163**, 107211 (2022). **This study provides significant insights into the fundamental deterioration mechanism of the fiber–matrix interface under coupled thermal–mechanical actions by performing debonding simulations**.
23. Ceroni, F., Cosenza, E., Gaetano, M. & Pecce, M. Durability issues of FRP rebars in reinforced concrete members. *Cement and Concr. Compos.* **28**, 857–868 (2006).
24. Lau, D., Büyüköztürk, O. & Buehler, M. J. Multiscale modeling of organic-inorganic interface: From molecular dynamics simulation to finite element modeling. *MRS Proc.* **1466** (2012). https://doi.org/10.1557/opl.2012.1427.
25. Liu, H. et al. Multiscale simulation study on the curing reaction and the network structure in a typical epoxy system. *Macromol.* **44**, 8650–8660 (2011).
26. Li, M. et al. Investigation the interphase formation process of carbon fiber/epoxy composites using a multiscale simulation method. *Compos. Sci. Technol.* **86**, 117–121 (2013).
27. Wu, Z., Wang, X., Zhao, X. & Noori, M. State-of-the-art review of FRP composites for major construction with high performance and longevity. *Int. J. Sustain. Mater. Struc. Syst.* **1**, 201–231 (2014).
28. Liu, T., Liu, X. & Feng, P. A comprehensive review on mechanical properties of pultruded FRP composites subjected to long-term environmental effects. *Compos. Part B: Eng.* **191**, 107958 (2020).
29. Blackburn, B. P., Tatar, J., Douglas, E. P. & Hamilton, H. R. Effects of hygrothermal conditioning on epoxy adhesives used in FRP composites. *Constr. Build. Mater.* **96**, 679–689 (2015).
30. Schutte, C. L. Environmental durability of glass-fiber composites. *Mater. Sci. Eng.: R: Rep.* **13**, 265–323 (1994).
31. Frigione, M., Aiello, M. A. & Naddeo, C. Water effects on the bond strength of concrete/concrete adhesive joints. *Constr. Build. Mater.* **20**, 957–970 (2006).
32. Frigione, M., Lettieri, M. & Mecchi, A. M. Environmental effects on epoxy adhesives employed for restoration of historical buildings1. *J. Mater. Civil Eng.* **18**, 715–722 (2006).
33. Deroiné, M. et al. Accelerated ageing of polylactide in aqueous environments: Comparative study between distilled water and seawater. *Polym. Degrad. Stab.* **108**, 319–329 (2014).
34. Carbas, R. J. C., Marques, E. A. S., da Silva, L. F. M. & Lopes, A. M. Effect of cure temperature on the glass transition temperature and mechanical properties of epoxy adhesives. *J. Adhes.* **90**, 104–119 (2014).
35. Dai, J.-G., Gao, W. Y. & Teng, J. G. Bond-slip model for FRP laminates externally bonded to concrete at elevated temperature. *J. Compos. Constr.* **17**, 217–228 (2013).
36. Da Silva, L. F., Öchsner, A. & Adams, R. D. *Handbook of adhesion technology*. (Springer Science & Business Media, 2011).
37. Feldman, D. Polymer weathering: Photo-oxidation. *J. Polym. Environ.* **10**, 163–173 (2002).
38. Iscen, A., Forero-Martinez, N. C., Valsson, O. & Kremer, K. Molecular simulation strategies for understanding the degradation mechanisms of acrylic polymers. *Macromolecules* **56**, 3272–3285 (2023).

39. Xu, T., Li, G. & Pang, S.-S. Effects of ultraviolet radiation on morphology and thermo-mechanical properties of shape memory polymer based syntactic foam. *Compos. Part A: Appl. Sci. Manuf.* **42**, 1525–1533 (2011).
40. Liau, W. B. & Tseng, F. P. The effect of long-term ultraviolet light irradiation on polymer matrix composites. *Polym. Compos.* **19**, 440–445 (1998).
41. Shokrieh, M. M. & Bayat, A. Effects of ultraviolet radiation on mechanical properties of glass/polyester composites. *J. Compos. Mater.* **41**, 2443–2455 (2007).
42. Nguyen, T.-C., Bai, Y., Zhao, X.-L. & Al-Mahaidi, R. Effects of ultraviolet radiation and associated elevated temperature on mechanical performance of steel/CFRP double strap joints. *Compos. Struct.* **94**, 3563–3573 (2012).
43. Dawood, M. & Rizkalla, S. Environmental durability of a CFRP system for strengthening steel structures. *Constr. Build. Mater.* **24**, 1682–1689 (2010).
44. Nguyen, T.-C., Bai, Y., Zhao, X.-L. & Al-Mahaidi, R. Durability of steel/CFRP double strap joints exposed to sea water, cyclic temperature and humidity. *Compos. Struct.* **94**, 1834–1845 (2012).
45. Wu, G., Wang, X., Wu, Z., Dong, Z. & Zhang, G. Durability of basalt fibers and composites in corrosive environments. *J. Compos. Mater.* **49**, 873–887 (2014).
46. Uthaman, A. et al. Durability of an epoxy resin and its carbon fiber- reinforced polymer composite upon immersion in water, acidic, and alkaline solutions. *Polymers* **12**, 614 (2020).
47. Guo, F., Al-Saadi, S., Singh Raman, R. K. & Zhao, X. L. Durability of fiber reinforced polymer (FRP) in simulated seawater sea sand concrete (SWSSC) environment. *Corros. Sci.* **141**, 1–13 (2018).
48. Mouzakis, D. E., Zoga, H. & Galiotis, C. Accelerated environmental ageing study of polyester/glass fiber reinforced composites (GFRPCs).*Compos. Part B: Eng.* **39**, 467–475 (2008).
49. Lu, T., Solis-Ramos, E., Yi, Y.-B. & Kumosa, M. Synergistic environmental degradation of glass reinforced polymer composites. *Polym. Degrad. Stab.* **131**, 1–8 (2016).
50. Lu, T., Solis-Ramos, E., Yi, Y. B. & Kumosa, M. Particle removal mechanisms in synergistic aging of polymers and glass reinforced polymer composites under combined UV and water. *Compos. Sci. Technol.* **153**, 273–281 (2017).
51. Zhurkov, S. N. Kinetic concept of the strength of solids. *Int. J. Fract. Mech.* **1**, 311–323 (1965).
52. Wang, Y. et al. A new thickness-based accelerated aging test methodology for resin materials: Theory and preliminary experimental study. *Constr. Build. Mater.* **186**, 986–995 (2018).
53. Davalos, J. F., Chen, A., Zahabi, M. & Ray, I. in *Earth and Space 2012* 722-731 (2012).
54. Sousa, J. M., Correia, J. R., Cabral-Fonseca, S. & Diogo, A. C. Effects of thermal cycles on the mechanical response of pultruded GFRP profiles used in civil engineering applications. *Compos. Struct.* **116**, 720–731 (2014).
55. Sun, P., Zhao, Y., Luo, Y. & Sun, L. Effect of temperature and cyclic hygrothermal aging on the interlaminar shear strength of carbon fiber/bismaleimide (BMI) composite. *Mater. Des.* **32**, 4341–4347 (2011).
56. Grammatikos, S. A., Jones, R. G., Evernden, M. & Correia, J. R. Thermal cycling effects on the durability of a pultruded GFRP material for off-shore civil engineering structures. *Compos. Struct.* **153**, 297–310 (2016).
57. Azwa, Z., Yousif, B., Manalo, A. & Karunasena, W. A review on the degradability of polymeric composites based on natural fibres. *Mater. Des.* **47**, 424–442 (2013).
58. Iglesias, J., González-Benito, J., Aznar, A., Bravo, J. & Baselga, J. Effect of glass fiber surface treatments on mechanical strength of epoxy based composite materials. *J. Colloid Interface Sci* **250**, 251–260 (2002).
59. Zhao, F. & Huang, Y. Grafting of polyhedral oligomeric silsesquioxanes on a carbon fiber surface: novel coupling agents for fiber/polymer matrix composites. *J. Mater. Chem.* **21**, 3695–3703 (2011).
60. Sever, K., Sarikanat, M., Seki, Y. & Tavman, I. H. Concentration effect of γ-glycidoxypropyltrimethoxysilane on the mechanical properties of glass fiber–epoxy composites. *Polym. Compos.* **30**, 1251–1257 (2009). **Effects of fiber treatment on mechanical properties and fracture behavior of glass fiber/epoxy composites were investigated experimentally**.
61. Mahmood, H., Tripathi, M., Pugno, N. & Pegoretti, A. Enhancement of interfacial adhesion in glass fiber/epoxy composites by electrophoretic deposition of graphene oxide on glass fibers. *Compos. Sci. Technol.* **126**, 149–157 (2016).
62. Liu, L. et al. Interfacial characterization, control and modification of carbon fiber reinforced polymer composites. *Compos. Sci. Technol.* **121**, 56–72 (2015). **This study shows that compared with the untreated composites, an obvious interphase with a thickness of 100 nm exists in the modified carbon fiber composites**.
63. Gibbs, J. W. *The scientific papers of J. Willard Gibbs, Volume 1: Thermodynamics*. Vol. 1 55-353 (Dover, 1961).
64. Cahn, J. W. & Hilliard, J. E. Free energy of a nonuniform system. I. Interfacial free energy. *J. Chem. Phys.* **28**, 258–267 (1958).
65. Cahn, J. W. On spinodal decomposition. *Acta Metall.* **9**, 795–801 (1961).
66. Chen, J.-L. & Chang, F.-C. Temperature-dependent phase behavior in poly(ϵ-caprolactone)–epoxy blends. *Polymer* **42**, 2193–2199 (2001).
67. Li, J., Du, Z., Li, H. & Zhang, C. Porous epoxy monolith prepared via chemically induced phase separation. *Polymer* **50**, 1526–1532 (2009).
68. Chung Hae, P. & Woo, L. Modeling void formation and unsaturated flow in liquid composite molding processes: a survey and review. *J. Reinforced Plast. Compos.* **30**, 957–977 (2011).
69. Suo, Z. & Lu, W. Forces that drive nanoscale self-assembly on solid surfaces. *J. Nanopart. Res.* **2**, 333–344 (2000).
70. Chen, L.-Q. Phase-field models for microstructure evolution. *Ann. Rev. Mater. Res.* **32**, 113–140 (2002).
71. Dona, K. N. G., Du, E., Carlsson, L. A., Fletcher, D. M. & Boardman, R. P. Modeling of water wicking along fiber/matrix interface voids in unidirectional carbon/vinyl ester composites. *Microfluidi. Nanofluid.* **24**, 31 (2020).
72. Weitsman, Y. J. *Fluid effects in polymers and polymeric composites*. (Springer Science & Business Media, 2011).
73. Gorbatkina, J. A. & Shaidurova, N. K. The effect of aging in water on the strength of fiber-polymer systems. *J. Adhes.* **35**, 203–215 (1991).
74. Lau, D. & Büyüköztürk, O. Fracture characterization of concrete/epoxy interface affected by moisture. *Mech. Mater.* **42**, 1031–1042 (2010).
75. Tuakta, C. & Büyüköztürk, O. Deterioration of FRP/concrete bond system under variable moisture conditions quantified by fracture mechanics. *Compos. Part B: Eng.* **42**, 145–154 (2011).
76. Wang, Z., Lin, K. & Zhao, Y.-P. The effect of sharp solid edges on the droplet wettability. *J. Colloid Interface Sci.* **552**, 563–571 (2019).
77. Laplace, P.-S. Theory of capillary attraction. *Supplements to the 10th book of Celestial Mechanics* (1807).
78. Churaev, N. V. & Sobolev, V. D. Prediction of contact angles on the basis of the Frumkin-Derjaguin approach. *Adv. Colloid Interf. Sci.* **61**, 1–16 (1995).
79. de Gennes, P. G. Wetting: statics and dynamics. *Rev. Mod. Phys.* **57**, 827–863 (1985).
80. Zhao, Y.-P. *Physical Mechanics of Surfaces and Interfaces*. (Science Press, 2012).
81. Lin, K. & Zhao, Y.-P. Mechanical peeling of van der Waals heterostructures: Theory and simulations. *Ext. Mech. Lett.* **30**, 100501 (2019).
82. Wei, Z., Lin, K., Wang, X. & Zhao, Y.-P. Peeling of graphene/molybdenum disulfide heterostructure at different angles: A continuum model with accommodations for van der Waals interaction. *Compos. Part A-Appl. S* **150**, 106592 (2021).
83. Lin, K., Huang, X. & Zhao, Y.-P. Combining image recognition and simulation to reproduce the adsorption/desorption behaviors of shale gas. *Energy Fuels* **34**, 258–269 (2019).
84. Lin, K. & Zhao, Y.-P. Entropy and enthalpy changes during adsorption and displacement of shale gas. *Energy* **221**, 119854 (2021).
85. Nguyen, M.-T. et al. Atomic origins of the self-healing function in cement–polymer composites. *ACS Appl. Mater. Interf.* **10**, 3011–3019 (2018).
86. Brenner, D. W. et al. A second-generation reactive empirical bond order (REBO) potential energy expression for hydrocarbons. *J. Phys. Condens. Matter*. **14**, 783–802 (2002).
87. Stuart, S. J., Tutein, A. B. & Harrison, J. A. A reactive potential for hydrocarbons with intermolecular interactions. *J. Chem. Phys.* **112**, 6472–6486 (2000).
88. van Duin, A. C. T., Dasgupta, S., Lorant, F. & Goddard, W. A. ReaxFF: A Reactive Force Field for Hydrocarbons. *J. Phys. Chem. A* **105**, 9396–9409 (2001).
89. Zhang, X. et al. Multi-objective parametrization of interatomic potentials for large deformation pathways and fracture of two-dimensional materials. *npj Comput. Mater.* **7**, 113 (2021).
90. Fonseca, G., Poltavsky, I., Vassilev-Galindo, V. & Tkatchenko, A. Improving molecular force fields across configurational space by combining supervised and unsupervised machine learning. *J. Chem. Phys.* **154**, 124102 (2021).
91. Buehler, M. J. & Ackbarow, T. Fracture mechanics of protein materials. *Mater. Today* **10**, 46–58 (2007).
92. Büyüköztürk, O., Buehler, M. J., Lau, D. & Tuakta, C. Structural solution using molecular dynamics: Fundamentals and a case study of epoxy-silica interface. *Int. J. Solids Struct.* **48**, 2131–2140 (2011).
93. Glasstone, S., Laidler, K. J. & Eyring, H. *The theory of rate processes*. (McGraw-hill, 1941).
94. Cherry, B. W. Kinetics of wetting of surfaces by polymers. *J. Colloid Interface Sci.* **29**, 174–176 (1969).
95. Hoffman, R. L. A study of the advancing interface: II. Theoretical prediction of the dynamic contact angle in liquid-gas systems. *J. Colloid Interf. Sci.* **94**, 470–486 (1983).
96. Vanlandingham, M. R., Eduljee, R. F. & Gillespie, J. W. Jr Moisture diffusion in epoxy systems. *J. Appl. Polym. Sci.* **71**, 787–798 (1999).
97. Jiang, X., Kolstein, H. & Bijlaard, F. S. K. Moisture diffusion in glass–fiber-reinforced polymer composite bridge under hot/wet environment. *Compos. Part B: Eng.* **45**, 407–416 (2013).

98. Berens, A. R. & Hopfenberg, H. B. Diffusion and relaxation in glassy polymer powders: 2. Separation of diffusion and relaxation parameters. *Polymer* **19**, 489–496 (1978).
99. Compte, A. & Metzler, R. The generalized Cattaneo equation for the description of anomalous transport processes. *J. Phys. A: Math. Gen.* **30**, 7277–7289 (1997).
100. Chen, J. K., Beraun, J. E. & Tzou, D. Y. A dual-phase-lag diffusion model for predicting thin film growth. *Semicond. Sci.Technol.* **15**, 235–241 (2000).
101. Hutchinson, J. M. Physical aging of polymers. *Progr. Polym. Sci.* **20**, 703–760 (1995).
102. Zheng, N. et al. In-situ pull-off of ZnO nanowire from carbon fiber and improvement of interlaminar toughness of hierarchical ZnO nanowire/carbon fiber hydrid composite laminates. *Carbon* **110**, 69–78 (2016).
103. Zheng, N. et al. Adhesion force measured by atomic force microscopy for direct carbon fiber-epoxy interfacial characterization. *Mater. Des.* **145**, 218–225 (2018).
104. Cordeiro, R. M. Reactive oxygen species at phospholipid bilayers: Distribution, mobility and permeation. *Biochimica et Biophysica Acta (BBA) - Biomembranes* **1838**, 438–444 (2014).
105. Nie, L., Burgess, A. & Ryan, A. Moisture permeation in liquid crystalline epoxy thermosets. *Macromol. Chem. Phys.* **214**, 225–235 (2013).
106. Heshmati, M., Haghani, R. & Al-Emrani, M. Effects of moisture on the long-term performance of adhesively bonded FRP/steel joints used in bridges. *Compos. Part B: Eng.* **92**, 447–462 (2016).
107. Scott, P. & Lees, J. Water, salt water, and alkaline solution uptake in epoxy thin films. *J. Appl. Polym. Sci.* **130**, 1898–1908 (2013).
108. Gao, Y. et al. Study on liquids diffusion into and relevant corrosion behaviour of glass fibre reinforced polymer used in high voltage composite insulator. *High Voltage* **5**, 53–61 (2020).
109. Lomov, S. V. et al. Meso-FE modelling of textile composites: Road map, data flow and algorithms. *Compos. Sci. Technol.* **67**, 1870–1891 (2007).
110. Koloor, S., Khosravani, M. R., Hamzah, R. & Tamin, M. FE model-based construction and progressive damage processes of FRP composite laminates with different manufacturing processes. *Int. J. Mech. Sci.* **141**, 223–235 (2018).
111. Ullah, Z., Kaczmarczyk, L. & Pearce, C. J. Three-dimensional nonlinear micro/meso-mechanical response of the fibre-reinforced polymer composites. *Compos. Struct.* **161**, 204–214 (2017).
112. Ken-Ichi, K. Distribution of directional data and fabric tensors. *Int. J. Eng. Sci.* **22**, 149–164 (1984).
113. Bauer, J. K. & Böhlke, T. Fiber orientation distributions based on planar fiber orientation tensors of fourth order. *Math. Mech. Solids* **28**, 773–794 (2023).
114. Eik, M., Puttonen, J. & Herrmann, H. The effect of approximation accuracy of the orientation distribution function on the elastic properties of short fibre reinforced composites. *Compos. Struct.* **148**, 12–18 (2016).
115. Reinold, J., Gudžulić, V. & Meschke, G. in *Computational Modelling of Concrete and Concrete Structures* 202-211 (CRC Press, 2022).
116. Jin, Z.-H. & Sun, C. Cohesive zone modeling of interface fracture in elastic bi-materials. *Eng. Fract. Mech.* **72**, 1805–1817 (2005).
117. Maitra, J. & Shukla, V. K. Cross-linking in hydrogels-a review. *Am. J. Polym. Sci* **4**, 25–31 (2014).
118. Yarovsky, I. & Evans, E. Computer simulation of structure and properties of crosslinked polymers: application to epoxy resins. *Polymer* **43**, 963–969 (2002).
119. Wu, C. & Xu, W. Atomistic molecular modelling of crosslinked epoxy resin. *Polymer* **47**, 6004–6009 (2006).
120. Shokuhfar, A. & Arab, B. The effect of cross linking density on the mechanical properties and structure of the epoxy polymers: molecular dynamics simulation. *J. Mol. Model* **19**, 3719–3731 (2013).
121. Okabe, T., Oya, Y., Tanabe, K., Kikugawa, G. & Yoshioka, K. Molecular dynamics simulation of crosslinked epoxy resins: Curing and mechanical properties. *Eur. Polym. J.* **80**, 78–88 (2016).
122. Sharp, N., Li, C., Strachan, A., Adams, D. & Pipes, R. B. Effects of water on epoxy cure kinetics and glass transition temperature utilizing molecular dynamics simulations. *J. Polym. Sci. Part B: Polym. Phys.* **55**, 1150–1159 (2017).
123. Unger, R. et al. Molecular modelling of epoxy resin crosslinking experimentally validated by near-infrared spectroscopy. *Comp. Mater. Sci.* **161**, 223–235 (2019).
124. Doherty, D. C., Holmes, B. N., Leung, P. & Ross, R. B. Polymerization molecular dynamics simulations. I. Cross-linked atomistic models for poly(methacrylate) networks. *Comput. Theor. Polym. Sci.* **8**, 169–178 (1998).
125. Wu, C. & Xu, W. Atomistic molecular simulations of structure and dynamics of crosslinked epoxy resin. *Polymer* **48**, 5802–5812 (2007).
126. Heine, D. R., Grest, G. S., Lorenz, C. D., Tsige, M. & Stevens, M. J. Atomistic simulations of end-linked poly(dimethylsiloxane) networks: structure and relaxation. *Macromolecules* **37**, 3857–3864 (2004).
127. Varshney, V., Patnaik, S. S., Roy, A. K. & Farmer, B. L. A molecular dynamics study of epoxy-based networks: cross-linking procedure and prediction of molecular and material properties. *Macromolecules* **41**, 6837–6842 (2008).
128. Vashisth, A., Ashraf, C., Zhang, W., Bakis, C. E. & van Duin, A. C. T. Accelerated ReaxFF simulations for describing the reactive cross-linking of polymers. *J. Phys. Chem. A* **122**, 6633–6642 (2018).
129. Ito, A. & Nakamura, H. Molecular dynamics simulation of bombardment of hydrogen atoms on graphite surface. *Commun. Comput. Phys.* **4**, 592–610 (2008).
130. Demir, B. et al. A predictive model of interfacial interactions between functionalised carbon fibre surfaces cross-linked with epoxy resin. *Compos. Sci. Technol.* **159**, 127–134 (2018).
131. Luo, T. & Lloyd, J. R. Enhancement of thermal energy transport across graphene/graphite and polymer interfaces: a molecular dynamics study. *Adv. Funct. Mater.* **22**, 2495–2502 (2012).
132. Shiu, S.-C. & Tsai, J.-L. Characterizing thermal and mechanical properties of graphene/epoxy nanocomposites. *Compos. Part B: Eng.* **56**, 691–697 (2014).
133. Salahshoor, H. & Rahbar, N. Nano-scale fracture toughness and behavior of graphene/epoxy interface. *J. Appl. Phys.* **112**, 023510 (2012).
134. Grujicic, M. et al. Filament-level modeling of aramid-based high-performance structural materials. *J. Mater. Eng. Perf.* **20**, 1401–1413 (2011).
135. Thiruppukuzhi, S. V. & Sun, C. T. Models for the strain-rate-dependent behavior of polymer composites. *Compos. Sci. Technol.* **61**, 1–12 (2001).
136. Zhandarov, S. & Mäder, E. Characterization of fiber/matrix interface strength: applicability of different tests, approaches and parameters. *Compos. Sci. Technol.* **65**, 149–160 (2005).
137. Bank, L. C., Gentry, T. R., Thompson, B. P. & Russell, J. S. A model specification for FRP composites for civil engineering structures. *Constr. Build. Mater.* **17**, 405–437 (2003).
138. Zhang, M., Jiang, B., Chen, C., Drummer, D. & Zhai, Z. The effect of temperature and strain rate on the interfacial behavior of glass fiber reinforced polypropylene composites: a molecular dynamics study. *Polymers (Basel)* **11**, 1766 (2019).
139. Niuchi, T., Koyanagi, J., Inoue, R. & Kogo, Y. Molecular dynamics study of the interfacial strength between carbon fiber and phenolic resin. *Adv. Compos. Mater.* **26**, 569–581 (2017).
140. Wang, H. et al. Effect of fiber surface functionalization on shear behavior at carbon fiber/epoxy interface through molecular dynamics analysis. *Compos. Part A: Appl. Sci. Manufact.* **126**, 105611 (2019).
141. Tam, L.-h, Jiang, J., Yu, Z., Orr, J. & Wu, C. Molecular dynamics investigation on the interfacial shear creep between carbon fiber and epoxy matrix. *Appl. Surf. Sci.* **537**, 148013 (2021).
142. Jian, W., Tam, L.-h & Lau, D. Atomistic study of interfacial creep behavior in epoxy-silica bilayer system. *Compos. B Eng.* **132**, 229–236 (2018).
143. Scott, D. W., Lai, J. S. & Zureick, A.-H. Creep behavior of fiber-reinforced polymeric composites: a review of the technical literature. *J. Reinf. Plast. Compos.* **14**, 588–617 (1995).
144. Tam, L.-h, Ntjam Minkeng, M. A., Lau, D., Mansour, W. & Wu, C. Molecular interfacial shearing creep behavior of carbon fiber/epoxy matrix interface under moisture condition. *Eng. Fract. Mech.* **282**, 109177 (2023).
145. Leone, M., Matthys, S. & Aiello, M. A. Effect of elevated service temperature on bond between FRP EBR systems and concrete. *Compos. Part B: Eng.* **40**, 85–93 (2009).
146. Yu, B. & Kodur, V. Effect of temperature on strength and stiffness properties of near-surface mounted FRP reinforcement. *Compos. Part B: Eng.* **58**, 510–517 (2014).
147. Heshmati, M., Haghani, R. & Al-Emrani, M. Durability of bonded FRP-to-steel joints: Effects of moisture, de-icing salt solution, temperature and FRP type. *Compos. Part B: Eng.* **119**, 153–167 (2017).
148. Ghiassi, B., Marcari, G., Oliveira, D. V. & Lourenço, P. B. Water degrading effects on the bond behavior in FRP-strengthened masonry. *Compos. Part B: Eng.* **54**, 11–19 (2013).
149. Heshmati, M., Haghani, R. & Al-Emrani, M. Environmental durability of adhesively bonded FRP/steel joints in civil engineering applications: State of the art. *Compos. Part B: Eng.* **81**, 259–275 (2015).
150. Mourad, A.-H. I., Idrisi, A. H., Wrage, M. C. & Abdel-Magid, B. M. Long-term durability of thermoset composites in seawater environment. *Compos. B Eng.* **168**, 243–253 (2019).
151. Yaphary, Y. L., Yu, Z., Lam, R. H. W., Hui, D. & Lau, D. Molecular dynamics simulations on adhesion of epoxy-silica interface in salt environment. *Compos. B Eng.* **131**, 165–172 (2017).
152. Xie, Q. et al. Effect of liquid diffusion and segregation on GFRP insulation performance in typical hygrothermal environment. *Compos. B Eng.* **244**, 110152 (2022). **This study provides a basis for revealing the deterioration mechanism of GFRP insulation in different hygrothermal environments**.
153. Vukovic, F. & Walsh, T. R. Moisture ingress at the molecular scale in hygrothermal aging of fiber–epoxy interfaces. *ACS Appl. Mater. Interf.* **12**, 55278–55289 (2020). **This work introduces new insights regarding the molecular-level details of moisture ingress and spatial distribution of water in these materials during hygrothermal aging**.

154. Guha, R. D., Rahmani, F., Berkowitz, K., Pasquinelli, M. & Grace, L. R. Temporal evolution of the behavior of absorbed moisture in a damaged polymer-quartz composite: A molecular dynamics study. *Comp. Mater. Sci.* **214**, 111690 (2022).
155. Kmiecik, S. et al. Coarse-grained protein models and their applications. *Chem. Rev.* **116**, 7898–7936 (2016).
156. Kremer, K. & Grest, G. S. Dynamics of entangled linear polymer melts: A molecular-dynamics simulation. *J. Chem. Phys.* **92**, 5057–5086 (1990).
157. Leelaprachakul, T., Kubo, A. & Umeno, Y. Coarse-grained molecular dynamics simulation of polycarbonate deformation: dependence of mechanical performance by the effect of spatial distribution and topological constraints. *Polymers* **15**, 43 (2023).
158. Guseva, D. V. et al. Crosslinking mechanisms, structure and glass transition in phthalonitrile resins: Insight from computer multiscale simulations and experiments. *J. Polym. Sci. Part B: Polym. Phys.* **56**, 362–374 (2018).
159. Yagyu, H. et al. Simulation of mechanical properties of epoxy-based chemically amplified resist by coarse-grained molecular dynamics. *Polymer* **53**, 4834–4842 (2012).
160. Sliozberg, Y. R. et al. Effect of polymer solvent on the mechanical properties of entangled polymer gels: Coarse-grained molecular simulation. *Polymer* **54**, 2555–2564 (2013).
161. Shoji, N. et al. Effect of conversion on epoxy resin properties: Combined molecular dynamics simulation and experimental study. *Polymer* **254**, 125041 (2022). **The success of the CG-EP model suggests that bottom-up modeling of angular parameters is a helpful tool for analyzing epoxy resin systems**.
162. Zhang, L.-W., Ji, W.-M., Hu, Y. & Liew, K. M. Atomistic insights into the tunable transition from cavitation to crazing in diamond nanothread-reinforced polymer composites. *Research* **2020**, 7815462 (2020). **This study proposed a two-phase CG model which can efficiently represent the chain flexibility and interfacial interaction in composites**.
163. Wu, X., Aramoon, A. & El-Awady, J. A. Hierarchical multiscale approach for modeling the deformation and failure of epoxy-based polymer matrix composites. *J. Phys. Chem. B* **124**, 11928–11938 (2020). **The results from the CG-MD-informed FEM model were compared to conventional FEM simulations that assume uniform epoxy mechanical properties**.
164. Yamaleev, N. & Mohan, R. Effect of the phase transition on intra-tow flow behavior and void formation in liquid composite molding. *Int. J. Multiph. Flow* **32**, 1219–1233 (2006).
165. Pethrick, R. A. Positron annihilation—a probe for nanoscale voids and free volume? *Progr. Polym. Sci.* **22**, 1–47 (1997).
166. Dlubek, G., Hassan, E., Krause-Rehberg, R. & Pionteck, J. Free volume of an epoxy resin and its relation to structural relaxation: Evidence from positron lifetime and pressure-volume-temperature experiments. *Phys. Rev. E* **73**, 031803 (2006).
167. Davalos, J. F., Chen, Y. & Ray, I. Effect of FRP bar degradation on interface bond with high strength concrete. *Cement Concrete Compos.* **30**, 722–730 (2008).
168. Tan, W. & Martínez-Pañeda, E. Phase field predictions of microscopic fracture and R-curve behaviour of fibre-reinforced composites. *Compos. Sci. Technol.* **202**, 108539 (2021).
169. Johnston, J. P., Koo, B., Subramanian, N. & Chattopadhyay, A. Modeling the molecular structure of the carbon fiber/polymer interphase for multiscale analysis of composites. *Compos. Part B: Eng.* **111**, 27–36 (2017).
170. Thomason, J. The interface region in glass fibre-reinforced epoxy resin composites: 1. Sample preparation, void content and interfacial strength. *Composites* **7**, 467–475 (1995).
171. Harper, B., Staab, G. & Chen, R. A note on the effects of voids upon the hygral and mechanical properties of AS4/3502 graphite/epoxy. *J. Compos. Mater.* **21**, 280–289 (1987).
172. Mehdikhani, M., Gorbatikh, L., Verpoest, I. & Lomov, S. V. Voids in fiber-reinforced polymer composites: A review on their formation, characteristics, and effects on mechanical performance. *J. Compos. Mater.* **53**, 1579–1669 (2019).

Acknowledgements

We acknowledge Professor Tao Yu from The Hong Kong Polytechnic University for fruitful discussions and advice. We acknowledge the financial support provided by the Hong Kong Research Grants Council (Project No: T22-502/18-R), and the National Natural Science Foundation of China (12202461).

Author contributions

K.L. led the conceptualization and wrote the original manuscript. K.L. and Z.W. discussed and revised the manuscript. All authors contributed to the editing of the manuscript and have approved its final version.

Competing interests

The authors declare no competing interests.

Additional information

Supplementary information The online version contains supplementary material available at https://doi.org/10.1038/s43246-023-00391-2.

Correspondence and requests for materials should be addressed to Kui Lin or Zhanlong Wang.

Peer review information *Communications Materials* thanks the anonymous reviewers for their contribution to the peer review of this work. Primary Handling Editors: John Plummer. A peer review file is available.